Electronic Supporting Information

A Bexarotene-Attached Re(I) tricarbonyl complex for NADH Oxidation and ROS-mediated Cancer Phototherapy

Rajesh Kushwaha,[a] Virendra Singh,[b] Biplob Koch,*[b] Samya Banerjee,*[a]

a. Department of Chemistry, Indian Institute of Technology (BHU), Varanasi, Uttar Pradesh 221005, India. Email: samya.chy@itbhu.ac.in

b. Department of Zoology, Institute of Science, Banaras Hindu University, Varanasi, Uttar Pradesh 221005, India. Email: biplob@bhu.ac.in

Table of Contents

Materials:

Rhenium pentacarbonyl chloride, $Re(CO)_5Cl$, was purchased from Merck. Benzoic acid and Bexarotene were obtained from BLD Pharmatech Ltd. Toluene was purchased from SRL Chem. Diethyl-ether, Hexane, ethyl acetate, DCM, acetone, and ethanol were purchased from Hyma Synthesis Pvt. Ltd. 1,3-Diphenylisobenzofuran, 2',7'-Dichlorodihydrofluorescein diacetate (DCFHDA), and β-Nicotinamide adenine dinucleotide reduced disodium salt (β-NADH) were purchased from Sigma Aldrich. Dulbecco's Phosphate Buffered Saline (DPBS) was purchased from Sigma Aldrich. MCF-7, A549, and HEK-293 cell lines were procured from NCCS Pune India. Dulbecco's Modified Eagle Medium (DMEM) and 12-well cell culture plates were purchased from Genetix Pvt. Ltd. T-25 flask, and 96-well plates were obtained from Eppendorf. MTT (3-(4,5- Dimethylthiazol-2-yl)-2,5-Diphenyltetrazolium Bromide) was obtained from SRL. FBS (Fetal Bovine Serum), Trypsin-EDTA, and Penicillin-streptomycin were procured from Gibco. JC-1 dye was procured from Cayman USA, and Hoechst 33342 and PI (propidium iodide) were purchased from Lobachemie. The cell event caspase 3/7 activity assay kit was procured from Invitrogen, USA, through local vendors.

Instrumentation

Agilent Cary 60 UV-Vis spectrophotometer was used for recording the UV-Vis spectral data. SHIMAZU A40241 (S. No. 02692) spectrophotometer was used for emission spectral data. AVH D 500AVANCE III HD 500 MHz OneBay NMR (from BRUKER BioSpin INTERNATIONAL AG) and Avance Neo 600 MHz (Bruker India Scientific Model) were used to record NMR spectra. For IR data, we have used the PerkinElmer spectrum FT-IR instrument. The HRMS data were obtained from the maXis impact instrument. Luzchem visible light photoreactor (model LZC-1) (400-700 nm, 10 J cm^{-2}) was used for photo-irradiation. In the 3-(4,5-dimethylthiazol-2-yl)-2,5-diphenyltetrazolium bromide (MTT) assay, the absorbance value of formazan was recorded using a TECAN microplate reader, and the graph was plotted using Microsoft Excel. EVOS FL Fluorescence microscopy from Life Technologies was used for cell imaging.

Experimental Section:

General synthetic procedure:

To synthesize the precursor complexes, 1.0 equivalent of bathophenanthroline (bathophen) and 1.0 equivalent of $Re(CO)_5Cl$ were dissolved in 15 mL of Toluene. The reaction mixture was refluxed for around 4 h under inert conditions. After 1-1.5 h, precipitation formation was started. The precipitated complex was filtered, washed with hexane and Et_2O, and dried *in vacuo* over P_4O_{10}. [Re(bathophen)$(CO)_3Cl$] (1.0 eq.) was dissolved into an anhydrous THF (3 mL) solution in a vial. AgOTf (1.1 eq.) was added to the vial under dark conditions. The mixture was stirred at room temperature under dark conditions for ~2 hours. The mixture was filtered and the residue was washed with anhydrous THF (3 mL). The collected solution was introduced into a 50 mL round bottom flask, followed by the addition of benzoic acid (**Re1**)/bexarotene(**Re2**) (1.0 eq.) and anhydrous Et_3N (1.5 eq.). The resulting mixture was refluxed at 70 °C temperature for 12 hours, evaporated under vacuum and the residue was

purified by column chromatography on neutral alumina using methanol and DCM (1: 99, *v/v*) as eluent to afford the expected product as yellow-orangish solid.

Re1: Yellow solid. 58% yield. $C_{34}H_{21}N_2O_5Re$ (M.W. = 723.8 g/mol) calcd. C 56.42, H 2.92, N 3.87, found: C 56.59, H 3.12, N 3.76, HR-MS (m/z for $[M+H]^+$): calcd. 725.1086, found: 725.1072. UV-Vis spectral data were recorded in DMSO:H_2O (1:9, v/v) where λ_{max} = 380 nm ($\varepsilon = 0.88 \times 10^4$ $M^{-1}cm^{-1}$); 440 nm ($\varepsilon = 0.52 \times 10^4$ $M^{-1}cm^{-1}$). ^{1}H NMR (500 MHz, DMSO-d_6) δ (ppm): 9.59 (d, *J* = 5.3 Hz, 2H), 8.17 (s, 2H), 8.10 (d, *J* = 5.3 Hz, 2H), 7.76 – 7.71 (m, 4H), 7.70 – 7.63 (m, 6H), 7.24 – 7.15 (m, 3H), 7.07 (t, *J* = 7.7 Hz, 2H). ^{13}C NMR (125 MHz, DMSO-d_6) δ (ppm): 197.73, 193.86, 169.06, 169.06, 153.02, 149.97, 149.97, 146.18, 134.63, 134.48, 129.45, 129.19, 129.19, 128.49, 128.49, 127.91, 127.91, 127.25, 126.83, 126.83, 125.91, 124.92. FT-IR (cm^{-1}): 2010 (s, sh, assym. CO), 1905 (s, sh, assym. CO), 1875 (s, sh, assym. CO), 1614 (m, sh), 1342 (m, sh), 1258 (m, sh), 1010 (m, sh), 767 (s, sh), 704 (s, sh) [m, medium; s, strong; br, broad; sh, sharp, assym., asymmetric].

Re2: Yellow-orangish solid. 48% yield. $C_{51}H_{43}N_2O_5Re$ (M.W. = 950.1 g/mol) calcd. C 64.47, H 4.56, N 2.95, found: C 64.32, H 4.73, N 3.02, HR-MS (m/z for $[M+H]^+$): calcd. 951.2808, found: 951.2866. UV-Vis spectral data were recorded in DMSO:H_2O (1:9, v/v) where λ_{max} = 385 ($\varepsilon = 1.2\times10^4$ $M^{-1}cm^{-1}$); 442 nm ($\varepsilon = 0.71 \times 10^4$ $M^{-1}cm^{-1}$). ^{1}H NMR (600 MHz, DMSO-d_6) δ (ppm): 9.50 (t, *J* = 4.4 Hz, 2H), 8.05 (t, *J* = 2.4 Hz, 2H), 8.01 (t, *J* = 4.5 Hz, 2H), 7.65 – 7.55 (m, 10H), 7.11 – 7.05 (m, 2H), 6.96 (t, *J* = 2.2 Hz, 1H), 6.88 – 6.81 (m, 3H), 5.59 – 5.55 (m, 1H), 5.00 – 4.96 (m, 1H), 1.70 – 1.64 (m, 3H), 1.52 (s, 4H), 1.14 – 1.12 (m, 6H), 1.07 (t, *J* = 2.3 Hz, 6H). ^{13}C NMR (150 MHz, DMSO) δ (ppm): 198.87, 194.98, 169.97, 154.14, 151.08, 148.90, 147.30, 143.94, 142.35, 142.09, 138.48, 135.77, 134.75, 132.42, 130.32, 129.65, 129.60, 129.34, 128.38, 128.14, 127.57, 127.06, 126.14, 126.04, 125.82, 116.27, 40.40, 40.26, 40.12, 39.98, 39.84, 39.71, 39.57, 35.10, 35.07, 34.66, 34.02, 33.86, 32.05, 29.71, 29.46, 26.81, 22.55, 19.82. FT-IR (cm^{-1}): 2015 (s, sh, assym. CO), 1915 (s, sh, assym. CO), 1890 (s, sh, assym. CO), 1620 (m, sh), 1345 (m, sh), 760 (m, sh), 704 (s, sh) [s, strong; sh, sharp, assym., asymmetric].

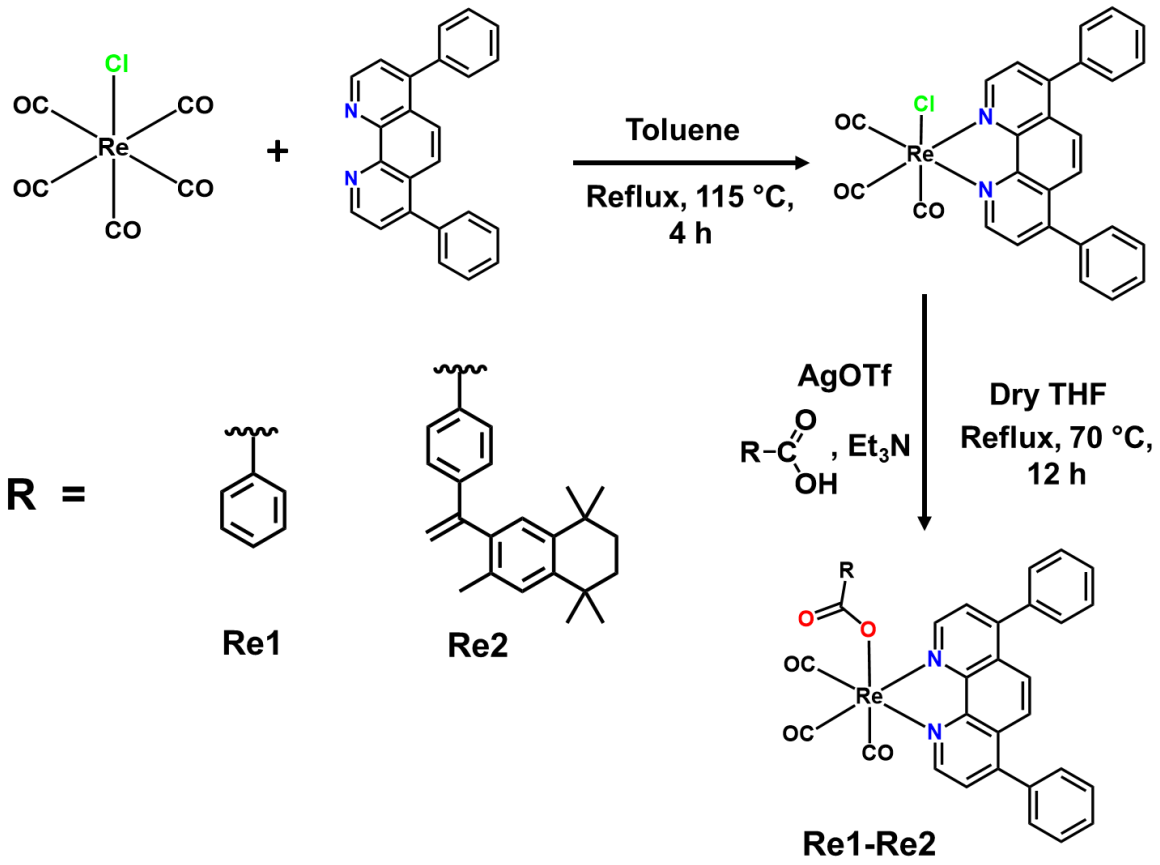

Reaction Scheme S1: Synthetic route for the synthesis of **Re1** and **Re2**.

Methods:

NMR spectroscopy

^{1}H and $^{13}C\{^{1}H\}$ NMR spectra were acquired using Bruker DPX 500 and Bruker Avance Neo 600 MHz (^{1}H = 500 MHz (**Re1**), 600 MHz (**Re2**) and $^{13}C\{^{1}H\}$ = 125 MHz (**Re1**), 150 MHz (**Re2**)) spectrometers. ^{1}H and $^{13}C\{^{1}H\}$ NMR spectra were recorded in DMSO-d_6. All data processing was carried out using MestReNova.

UV-Vis spectra

An Agilent Cary 60 UV-Vis spectrophotometer was used with 1 cm path-length quartz cuvettes. Spectra were processed using Origin Pro 2019 software. The UV-Vis spectra of **Re1** and **Re2** in DMSO:H_2O (1:9, v/v) were taken at 293 K from 250-700 nm. For pH experiments, the PBS of different pH values (i.e., 6, 7, 8) was used in place of water.

Emission spectra

The emission spectra of **Re2** (100 µM) in different DMSO-water (100:0 and 1:99, v/v) solutions were recorded with excitation at λex = 380 nm in a 1 cm quartz cuvette at room temperature.

Lipophilicity coefficient

The lipophilicity of **Re2** was determined by measuring its distribution coefficient between the octanol and water phases using the 'shake-flask' method.[1] For this procedure, the phases were pre-saturated with each other. The complex was initially dissolved in octanol (phase A), where it was predominantly present, with an absorbance of approximately 1.0 at 425 nm. This solution was then mixed with an equal volume of water (phase B), stirred at 600 rpm for 12 h, and allowed to equilibrate for 24 h. Phase A was carefully separated from phase B, and the concentration of **Re2** before and after mixing was measured using UV-Vis. absorption spectroscopy at 425 nm.

DFT Calculation

The density functional theory (DFT) and time-dependent DFT (TD-DFT) calculations were performed on neutral Re complexes using the Gaussian 16 revision A.03 quantum chemistry package.[2] For all calculations, the CAM-B3LYP function was used along with the CPCM solvation model in water. LANL2DZ with pseudo LANL2 basis set for Re and 6-31g* for other atoms was used for optimization.[3] The ground state (S_0) geometry of the complexes was carried out using restricted DFT, the first excited singlet state (S_1) geometry using TD-DFT, and the first excited triplet state (T_1) geometry using unrestricted DFT. The optimized S_0, S_1, and T_1 structures were confirmed to be local minima at the same computational level. FMOs were generated at the same level of theory. Natural transition orbitals (NTOs) were generated at the same level of theory.

$^{1}O_2$ generation

The $^{1}O_2$ generation was measured using the probe 1,3-Diphenylisobenzofuran (DPBF) upon light irradiation.[4] In brief, a DMSO:PBS solution (2:98 v/v, pH =7) containing 2 µM of **Re1** and **Re2** and 50 µM of DPBF was monitored by UV-vis spectroscopy after different durations of

light exposure (400-700 nm, 10 J cm^{-2}). For pH experiments, the PBS of different pH values (i.e., 6, 7, 8) was used. The absorbance at 419 nm was monitored for $^1O_2$ generation. The following equation determined the $^1O_2$ quantum yields (Φ_Δ) for **Re1** and **Re2**:

$$\phi_\Delta^S = \phi_\Delta^R \times (M_S/M_R)$$

where 'M' denotes the linear fit slope of the DPBF-based peak at 419 nm vs the time interval. "S" denotes the samples, and "R" denotes the standard, $Ru(bpy)_3Cl_2$.[5]

NADH Oxidation

Reactions between **Re1** and **Re2** (5 µM) and NADH (150 µM) in DMSO-PBS solution (2:98 v/v) were monitored by UV-Vis spectroscopy at ambient temperature in the dark or on irradiation with visible light (400-700 nm, 10 J cm^{-2}).[6] In control experiments, different known ROS scavengers (D-mannitol for radical-based ROS, and NaN3 for $^1O_2$, ~1mM) were added to the above solution.[6] The turnover number for NADH to NAD^+ oxidation was calculated using the following equations:

$$[NAD^+] = [\{Abs(339\ nm)_{initial} - Abs(339\ nm)_{final}\}/Abs(339\ nm)_{initial}] \times [NADH]$$

$$\text{Turnover number (TON)} = [NAD^+]/[\text{Catalyst}]$$

$$\text{Turnover frequency (TOF)} = \text{Turnover number/time (h)}$$

Molecular Docking

The molecular docking analysis of **Re1**, **Re2**, and bexarotene with the RXRα receptor (PDB ID: 1MVC) was performed using AutoDock 4.2 (MGL tools 1.5.7) with the previously reported protocol.[7,8] The energy-optimized structures were converted into .pdb format. Thereafter, these structures were converted to the ".pdbqt" format and docked with the respective proteins using the Autodock 4 software.[8] Different proteins were obtained in the ".pdb" format from the RCSB Protein Data Bank. Before docking, the protein structures were prepared by removing water molecules and other co-crystallized structures, adding polar hydrogens, and computing the Kollman charges. The docking for complexes and protein substituents was performed using Autodock 4 using the genetic search algorithm with genetic algorithm parameters set to 10 runs on a population size of 150. The maximum number of evaluations is set to 25000000 (long). The output was obtained as a Lamarckian GA format file containing information related to binding energies and docked conformers. The best-docked conformer data were extracted from the ".pdbqt" format and were analyzed using the Discovery Studios 9 software and PyMOL (Version 2) for 2D/3D interactions with the amino acids of the proteins.[9,10]

Cellular assays

MTT assay

Cytotoxicity assessments were conducted on MCF-7 cells (human breast adenocarcinoma cell line), A549 cells (human Lung cancer cell line), and HEK-293 cells (Human Embryonic Kidney cell line) to evaluate the cytotoxic effect of **Re1** and **Re2** by MTT assay.[11] 10000 cells/well of each type (MCF-7, A549, and HEK-293) were seeded in 2 different (one for light exposure, the second for dark conditions) 96-well plates in DMEM with 10% FBS and 1% penicillin-streptomycin solution, and placed in a 37 ℃, 5% CO_2 incubator for 24 h to equilibrate and allow cell attachment. After that, the medium was removed completely, and the fresh medium containing different concentrations of **Re1** and **Re2** (0.25 µM, 0.5 µM, 1 µM, 5 µM, 10 µM, 25 µM, and 50 µM) was added to each well, and kept for a 4 h incubation in a 5% humidified CO_2 incubator at 37˚C. The percentage of DMSO in the culture media was within the permissible limit (<1%). Thereafter, the drug-containing medium was discarded, and 100 µL PBS (phosphate buffer saline) was added to each well of all treated 96-well plates. One of those plates was exposed to light (Light source: 400-700 nm, 10 J cm^{-2}, 10 min), and subsequently, one was kept in a dark condition. After light irradiation, PBS was removed from both plates, and a fresh DMEM medium was added to each and incubated for another 20 h at 37 °C in a humidified 5% CO_2 incubator. Finally, the medium was discarded, and the fresh MTT-containing medium was added to each well. After 2 h of incubation, the MTT-containing medium was removed, and the formazan product was dissolved in 100 µL of DMSO and further incubated for 0.5 h. The cell viability was evaluated by measurement of the absorbance at 570 nm, using a multiplate reader. IC_{50} values were calculated from curves constructed by plotting cell survival (%) versus drug concentration (µM). All experiments were made in triplicate. Each experiment was performed in triplicate, and data were taken as the average of three independent sets of experiments.[11]

DCFDA assay

The assay was performed by seeding 0.5×10^5 MCF-7 cells/well in two 12-well cell culture plates (one for light exposure, the second one for dark conditions) followed by treatments with **Re2** at its light IC_{50} value concentration, and incubated for 4 h. After that, a fresh PBS was added to each well after discarding the drug-containing medium, and one plate was exposed to light (400-700 nm, 10 J cm^{-2}, 10 min), another one was kept in dark condition. After light irradiation, PBS was removed, and fresh DMEM was added to each plate and incubated for another 20 h. The cells underwent a PBS wash, followed by the addition of 10 µM DCFDA, followed by incubation at 37 °C for 0.5 h. Finally, images were photographed in a fluorescent microscope set to excitation at 450-490 nm and emission at 500-550 nm filters under green channels and phase contrast at 400X magnification.[12]

JC-1 assay

Approximately 0.5 × 10^5 MCF-7 cells/well in two 12-well cell culture plates (one for light exposure, the second one for dark conditions) were seeded and treated with **Re2** at light IC_{50} concentration and allowed to incubate in the dark at 37 °C for 6 h. The cells were subjected to a PBS wash after this incubation period. After that, one group of cells was exposed to light (400-700 nm, 10 J cm^{-2}, 10 min), while the other group remained in the dark. Cells were then incubated in fresh DMEM for 18 h. Finally, the medium was discarded, and the cells underwent a PBS wash. The cells were then stained using JC-1 dye to visualize changes. Fluorescence-emitting images were captured at 100X magnification (EVOS FL by Life Technology). For capturing images, excitation was done primarily at 488 nm, while emissions were detected at both 530 nm (green for monomers) and 595 nm (orange-red for aggregates).[13]

Detection of apoptosis by acridine orange/ethidium bromide dual staining

Acridine orange/ethidium bromide dual staining is generally used in the discrimination between live cells and apoptotic cells.[14,15] Acridine orange is permissible in all cells, staining nuclei with green emission. Ethidium bromide enters only dead cells with compromised membrane integrity, staining nuclei and emitting a yellowish-orange fluorescence.[9,10] Thus, live cells display normal green nuclei, early apoptotic cells show bright green or yellowish-orange nuclei with condensed or fragmented chromatin, late apoptotic cells display condensed and fragmented orange-red chromatin, and cells undergoing necrosis exhibit structurally intact deep orange nuclei.[14,15] Briefly, 0.5 × 10^5 MCF-7 cells/well were seeded in 12-well cell culture plates. The cells were then treated with **Re2** at the light IC_{50} concentration and processed using the abovementioned method. The cells were washed with PBS and stained with acridine orange and ethidium bromide at 10 µg mL^{-1} concentration, followed by 30 min incubation at 37 °C. The images were captured using a fluorescence microscope (100X) under red and green channels. The images were recorded at 488 nm excitation/525 nm emission for AO, and 488 nm excitation/616-635 nm emission for EB.

Detection of apoptosis by AnnexinV/FITC and PI assay

To examine apoptosis, quantitative flow cytometry analysis was performed on MCF-7 cells after treatments with **Re2** at the light IC_{50} concentration and processed as mentioned above. After the final incubation, cells were harvested in PBS with 1 mM EDTA (pH 7.4). Further, treated and control cells were processed according to the manufacturer's protocol for Alexa Fluor 488 Annexin V/PI staining (Thermo Fisher Scientific, Invitrogen Bioservices India Pvt. Ltd.). After staining, the samples were examined by Beckman Coulter.

Caspase-3/7 assay

To perform the caspase 3/7 assay, 0.5×10^5 MCF-7 cells/well were seeded in two separate 24-well culture plates (one for light exposure, the second one for dark conditions), treated with the light IC_{50} concentration of **Re2**, and incubated for 12 h. After incubation, the **Re2**-containing medium was removed from each well. PBS was added to each well of both plates; one plate was exposed to light irradiation (400-700 nm, 10 J cm^{-2} , 10 min), and another was kept in a dark condition. Cells were then incubated in fresh DMEM for 12 h. After 12 h incubation, the cells were collected and stained with caspase 3/7 and sytox according to the manufacturer protocol (CellEvent™ Caspase-3/7 Green Flow Cytometry Assay Kit by thermoScientific). Finally, the images were captured in green, red, and phase contrast channels through an EVOS FL microscope at 100X magnification equipped with a 488-nm laser. The green fluorescence emission was collected using a 530 nm bandpass filter for CellEvent™ Caspase-3/7 Green detection reagent, and a red fluorescence emission was collected at a 690 nm bandpass filter for SYTOX™ AADvanced™ Dead Cell Stain, respectively.[15]

Statistical analysis

The outcome of the results was expressed as mean ± standard error of the three independent repeated experiments. Sample size i.e., n = 3, was used for respective statistical analysis. The statistical analysis was conducted utilizing SPSS 16.0 (SPSS, Chicago, IL, USA) software. Results were compared between the dark control with the rest of the group (**Re2**, Control light, and **Re2** + light). The statistical analysis was done by One-way ANOVA followed by Tukey's Post Hoc Test. Values of $p < 0.05$ were considered statistically significant.

Tables:

Table S1. Crystal data parameters and refinement details of **Re1**.

Entry	**Re1**
Empirical formula	$C_{34}H_{21}N_2O_5Re$
Formula weight	723.73
Temperature/K	298
Crystal system	monoclinic
Space group	$P2_1/n$
a/Å	9.99340(10)
b/Å	14.89530(10)
c/Å	18.55280(10)

α/°	90
β/°	97.4900(10)
γ/°	90
Volume/Å^3	2738.11(4)
Z	4
ρ_{calc}g/cm^3	1.756
μ/mm^{-1}	9.077
F(000)	1416.0
Crystal size/mm^3	0.3 × 0.2 × 0.2
Radiation	Cu K_α (λ = 1.54184)
2Θ range for data collection/°	7.638 to 136.194
Index ranges	-7 ≤ h ≤ 12, -17 ≤ k ≤ 17, -22 ≤ l ≤ 22
Reflections collected	50545
Independent reflections	4953 [R_{int} = 0.0446, R_{sigma} = 0.0186]
Data/restraints/parameters	4953/0/379
Goodness-of-fit on F^2	1.150
Final R indexes [I>=2σ (I)]	R_1 = 0.0376, wR_2 = 0.1181
Final R indexes [all data]	R_1 = 0.0396, wR_2 = 0.1189
Largest diff. peak/hole / e Å^{-3}	1.65/-0.69
CCDC	**2463073**

Table S2: Selected bond lengths (Å) and bond angles (°) of **Re1**.

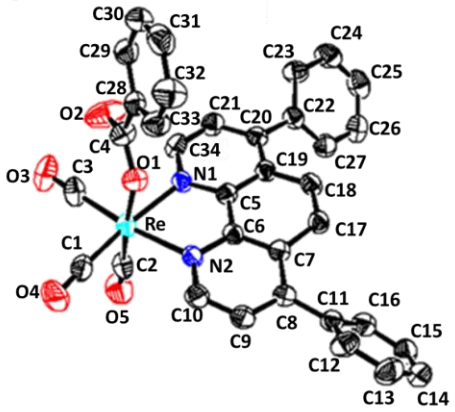

Bond Lengths			
Bond(s)	**Distances**	**Bond(s)**	**Distances**
Re-N1	2.189(5)	**Re-C1**	1.909(8)
Re-O1	2.128(5)	**Re-C2**	1.908(9)
Re-N2	2.179(6)	**Re-C3**	1.926(9)
Bond Angles			
N1-Re-O1	83.4(2)	**C1-Re-C2**	87.0(4)
N1-Re-N1	74.9(2)	**C1-Re-C3**	89.7(4)
N1-Re-C1	173.0(3)	**C2-Re-C3**	86.6(4)
N1-Re-C2	95.0(3)	**O1-Re-N2**	81.5(2)
N1-Re-C3	97.1(3)	**O1-Re-C1**	94.2(3)
N2-Re-C1	98.3(3)	**O1-Re-C2**	176.2(3)
N2-Re-C2	94.8(3)	**O1-Re-C3**	97.0(3)
N2-Re-C3	171.9(3)	**Re-O1-C4**	122.2(5)
Torsion Angles			
C21-C20-C22-C27	131.4(8)	**C12-C11-C8-C7**	138.3(8)
C21-C20-C22-C23	46(1)	**C12-C11-C8-C9**	44(1)
C19-C20-C22-C23	138.1(8)	**C16-C11-C8-C7**	44(1)
C19-C20-C22-C27	45(1)	**C16-C11-C8-C9**	133.8(8)

Table S3. Computed frontier molecular orbital (FMO) energies for **Re1** and **Re2** in ground state (S_0) using CAM-B3LYP/LANL2DZ/6-31g* level of theory in water.

	HOMO (eV)	LUMO (eV)	HOMO-LUMO gap (eV)
Re1	-6.87	-1.48	5.40
Re2	-6.86	-1.49	5.37

Table S4: Energy (eV) of the lowest singlet and triplet ($S_0 \rightarrow S_n/T_n$; n = 1 to 10) transitions for **Re1** at CAM-B3LYP/LANL2DZ/6-31g* level of theory in water.

States	Singlets		Triplets[b]
	eV	Oscillator Stregth	eV
1	3.62	0.1591	2.55
2	3.69	0.0472	2.98
3	4.05	0.0027	3.40
4	4.06	0.2049	3.41
5	4.18	0.0588	3.47
6	4.30	0.0814	3.50
7	4.35	0.0057	3.69
8	4.46	0.0021	3.77
9	4.50	0.0487	3.91
10	4.53	0.0628	3.93

[b]Calculating the oscillator strengths is beyond the scope of the theory used.

Table S5: Energy (eV) of the lowest singlet and triplet ($S_0 \rightarrow S_n/T_n$; n = 1 to 10) transitions of **Re2** at CAM-B3LYP/LANL2DZ/6-31g* level of theory in water.

States	Singlets		Triplets[b]
	eV	Oscillator Stregth	eV
1	3.62	0.1557	2.55
2	3.70	0.0451	2.81
3	4.04	0.0030	2.98
4	4.05	0.1994	3.33
5	4.08	0.0545	3.41
6	4.30	0.0814	3.47
7	4.35	0.0067	3.50
8	4.45	0.0023	3.69
9	4.50	0.0529	3.77
10	4.53	0.0521	3.84

[b]Calculating the oscillator strengths is beyond the scope of the theory used.

Table S6: IC_{50} values (μM), photo-cytotoxicity index (PI, PI = IC_{50} dark/IC_{50} light), Selectivity Index (SI, SI = $IC_{50\ normal\ cells}$ light / $IC_{50\ cancer\ cells}$ light) of **Re1** and **Re2**, and cisplatin.

	A549 Cells				MCF-7 cells				HEK-293 cells	
	Dark	**Light**	**PI**	**SI**	**Dark**	**Light**	**PI**	**SI**	**Dark**	**Light**
Re1[a]	> 50	12.01 ± 1.80	> 4.2		21.80 ± 0.25	3.91 ± 0.13	5.6	-	-	-
Re2[a]	36.18 ± 1.94	1.02 ± 0.12	35.4	> 49	19.20 ± 0.86	0.27 ± 0.06	71.1	> 185	> 50	> 50
CisPlatin[b]	8.3 ± 1.2	8.6 ± 0.9	1.1	-						

[a]Visible light irradiation (400-700 nm, 10 J cm^{-2}). Light treatment: Incubation time: 6 h, Light irradiation for 10 min. Recovery time: 18 h. Dark treatment: Incubation time: 6 h, Recovery time: 18 h. [b]Cells were treated with cisplatin, kept in the dark, or received irradiation after 4 h incubation without replacing the medium, and following 44 h incubation (from ref. 6).

Table S7. Binding energy, hydrogen bonding, and hydrophobic interaction of **Re1**, **Re2**, and bexarotene with RXRα receptor (PDB ID: 1MVC) obtained by molecular docking.

Complex	Binding Energy (Kcal/mol)	Hydrogen Bonding	Hydrophobic interactions
Re1	-8.85	-	THR A:449; ARG A:302; GLU A:453; MET A:454; LEU A:301; VAL A:298; LEU A:294; LYS A:284; VAL A:280; PHE A:277; GLU A:281; PHEN A:450
Re2	-10.94	ARG A:316	PRO A:244; GLU A:243; SER A:312; LEU A:367; GLU A:239; LYS A:364; HIS A:315; ASP A:363; MET A:362; ILE A:318; LEU A:325; ALA:319; HIS A:331; VAL A:320; LYS A:321
Bexarotene	-12.36	ARG A:316; ALA A:327	VAL A:265,342,349; ILE A:345,324,268; PHE A:439,313,346; HIS A:435; CYS A:432,269; ALA A:271, 272; LEU A:309,326,451; ASN A:306; GLN A:275

Figures:

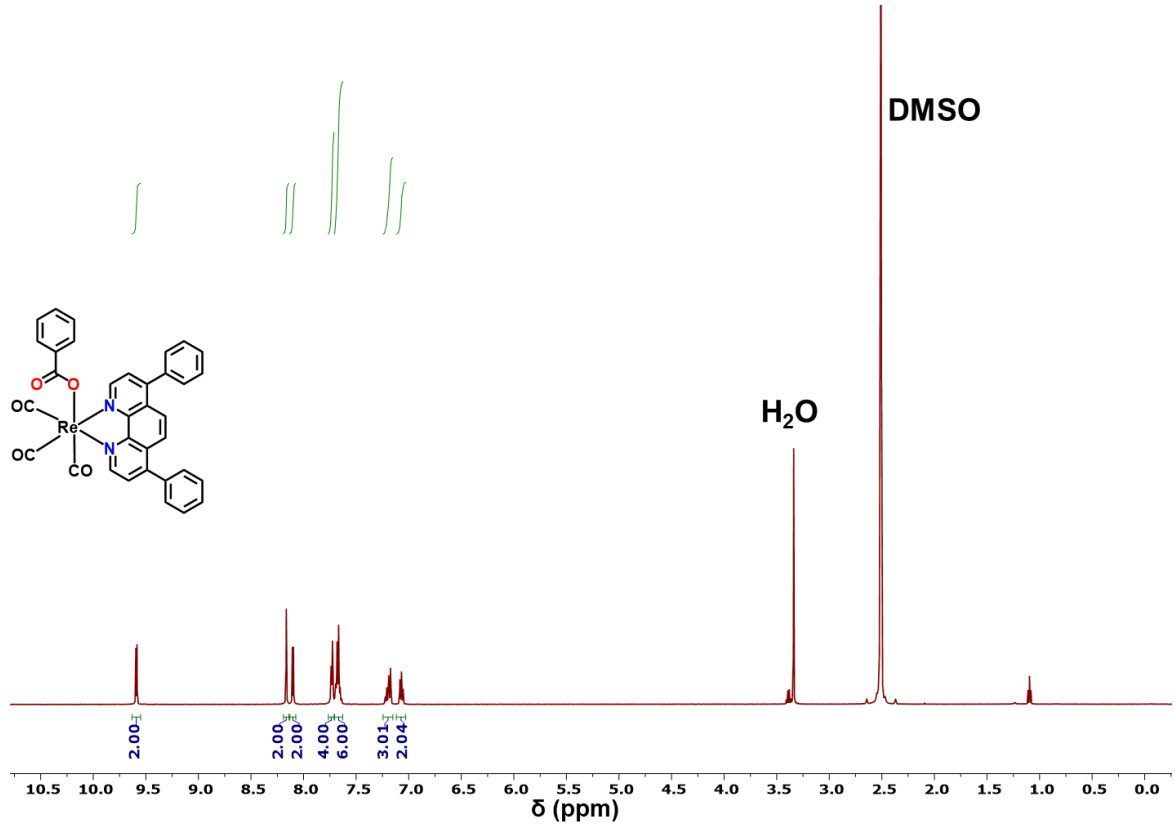

Figure S1: ^{1}H NMR of **Re1** in DMSO-d_6 (500 MHz).

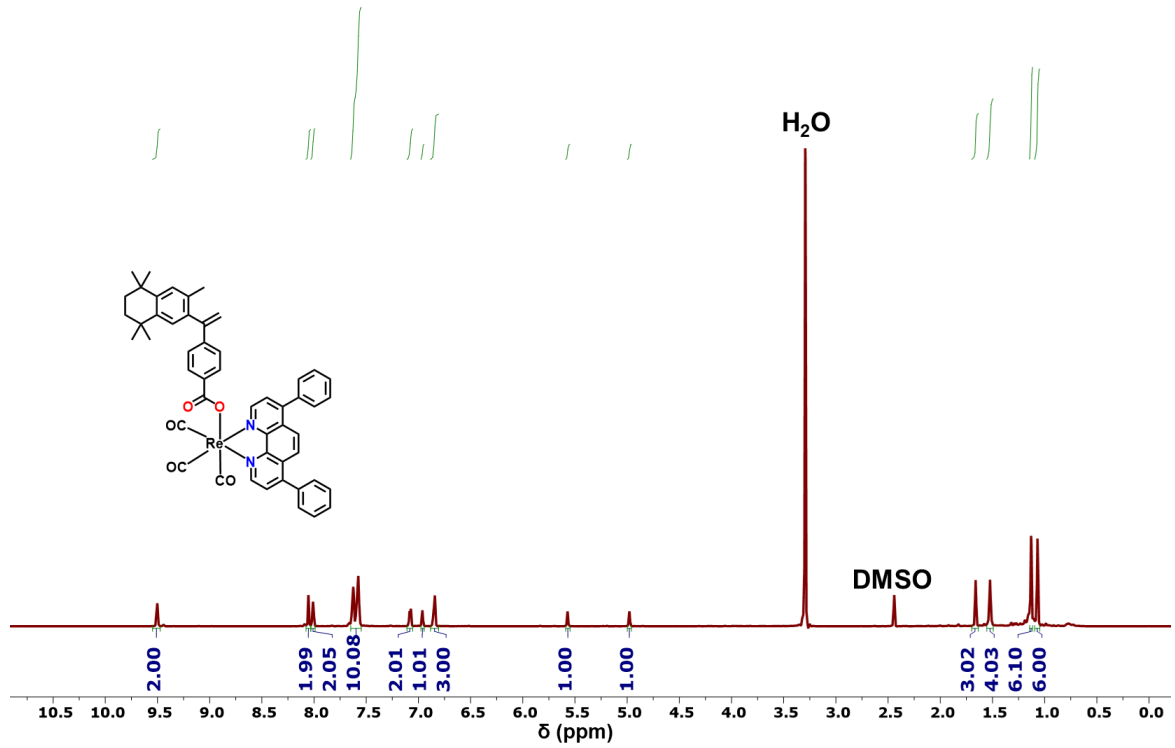

Figure S2: ^{1}H NMR of **Re2** in DMSO-d_6 (600 MHz).

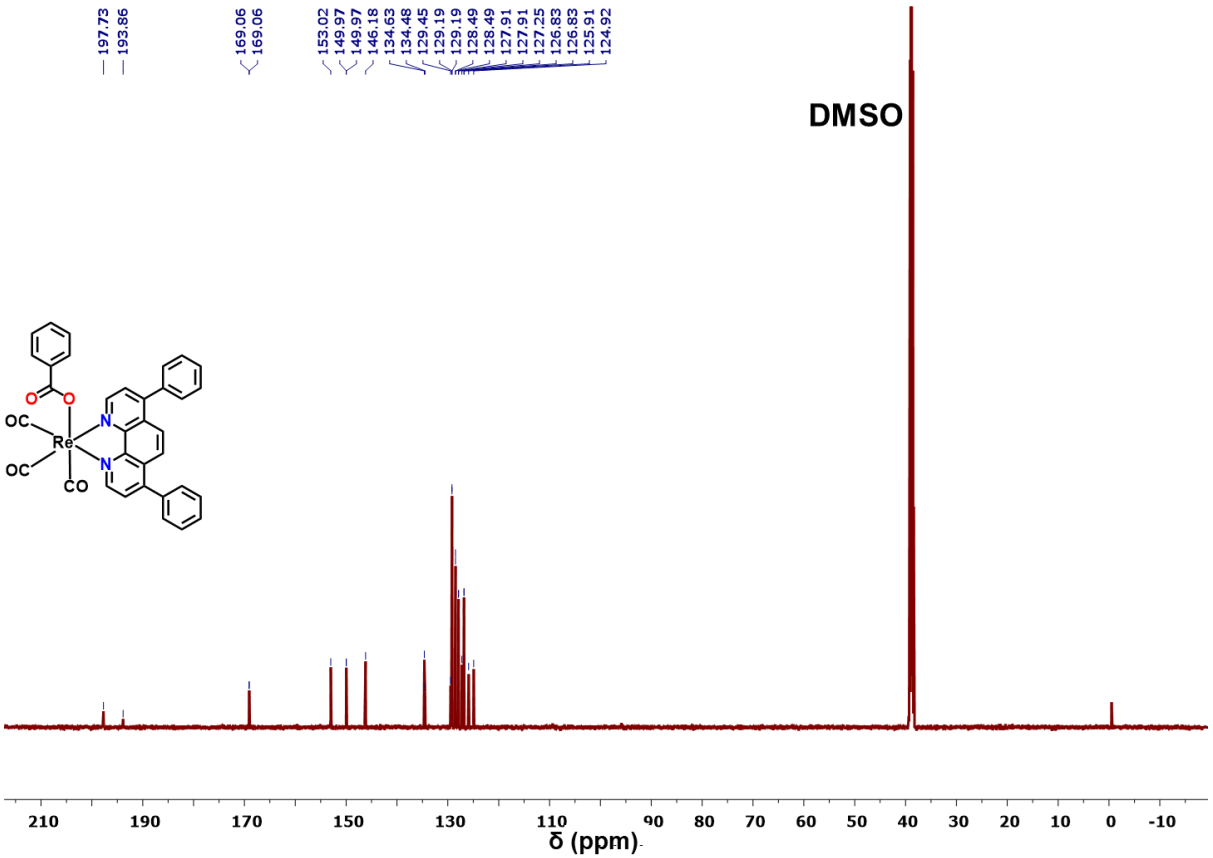

Figure S3: $^{13}C\{^{1}H\}$ NMR of **Re1** in DMSO-d_6 (125 MHz).

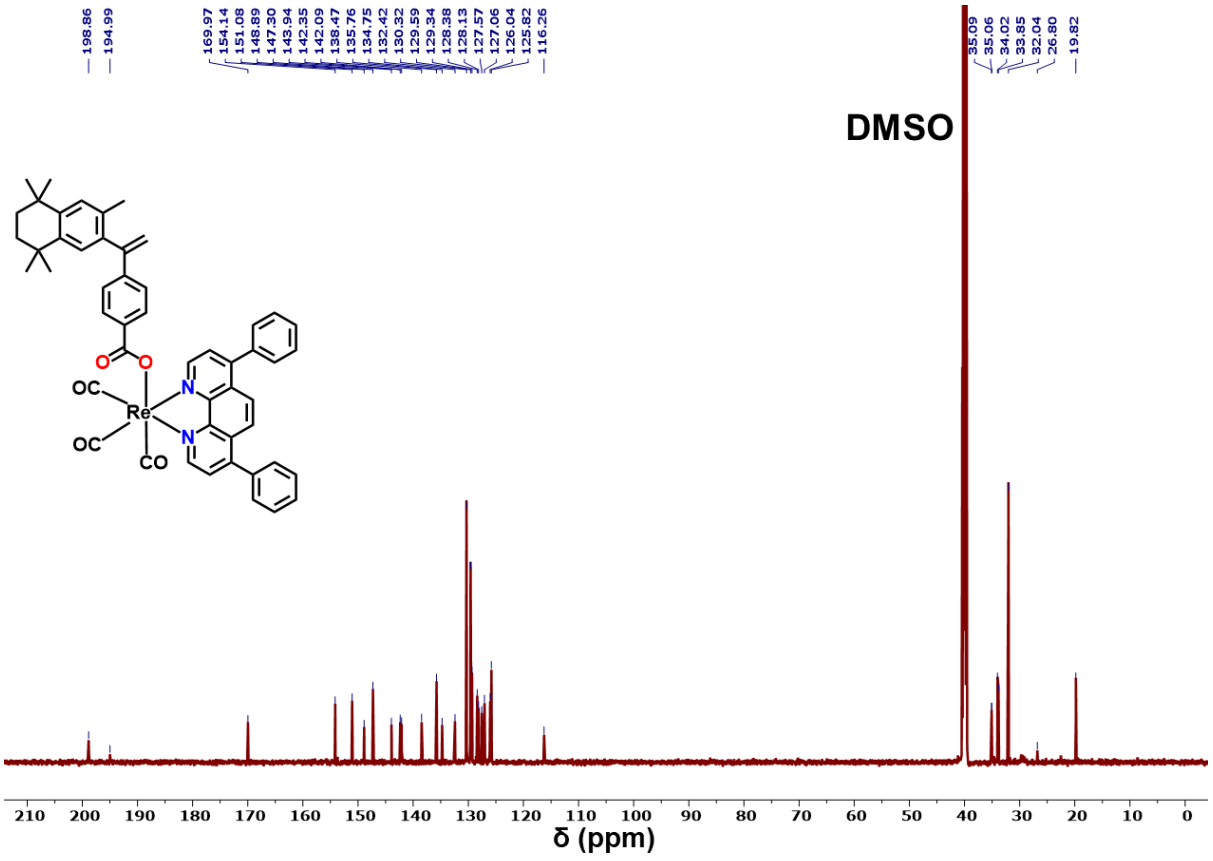

Figure S4: $^{13}C\{^{1}H\}$ NMR of **Re2** in DMSO-d_6 (150 MHz).

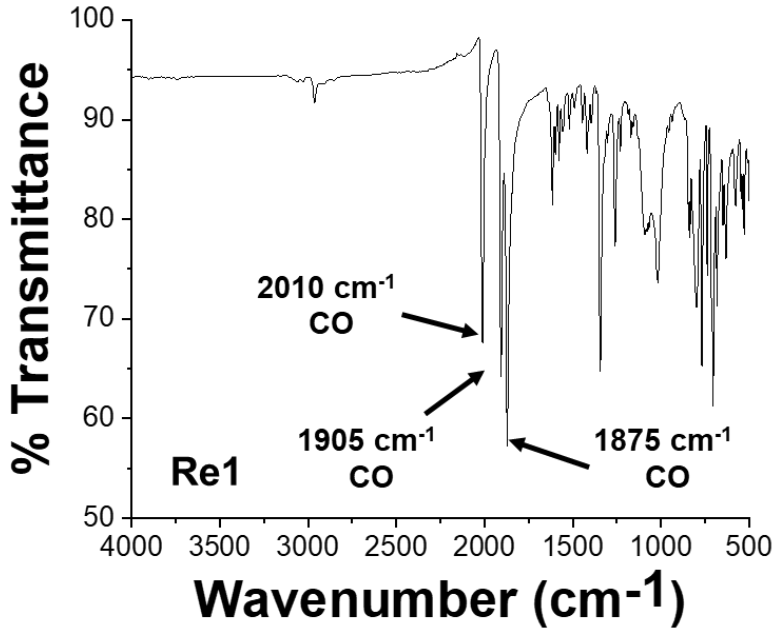

Figure S5: FT-IR spectra of **Re1**.

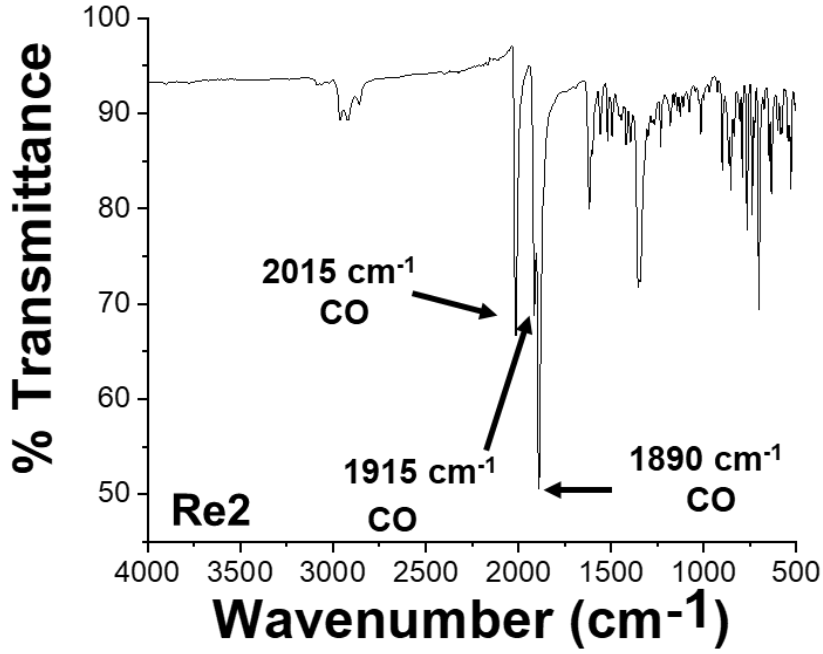

Figure S6: FT-IR spectra of **Re2**.

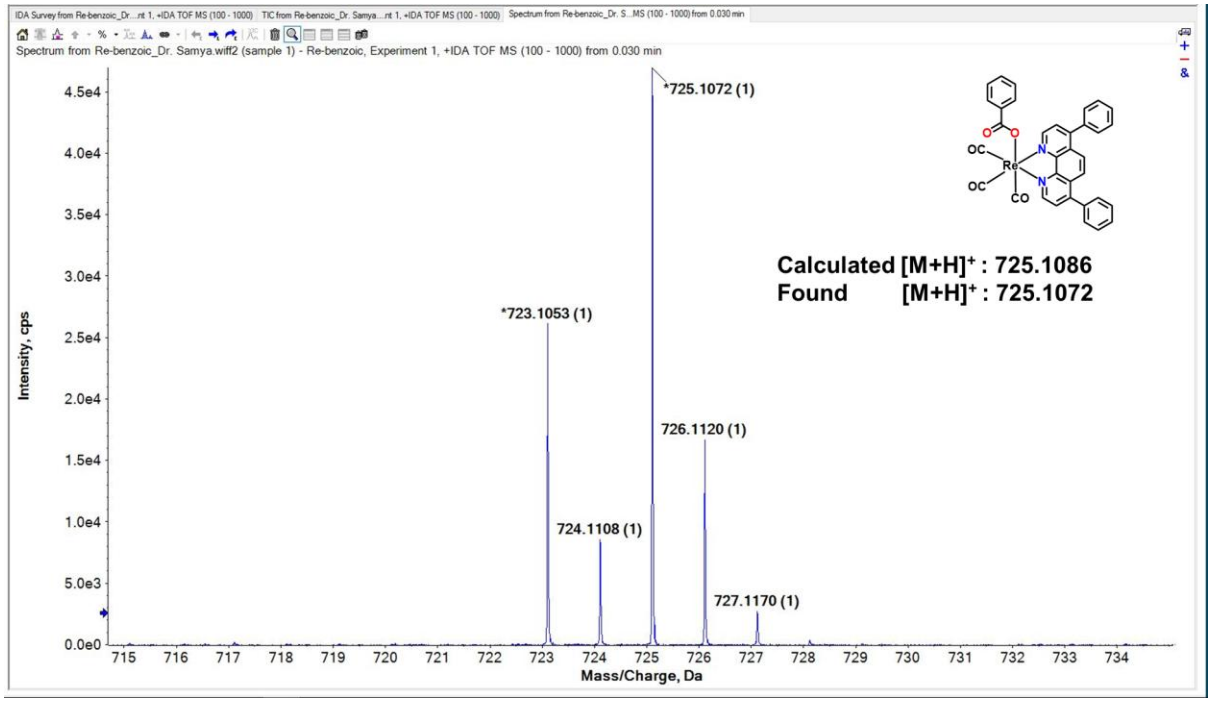

Figure S7: HRMS of **Re1** in CH_3OH.

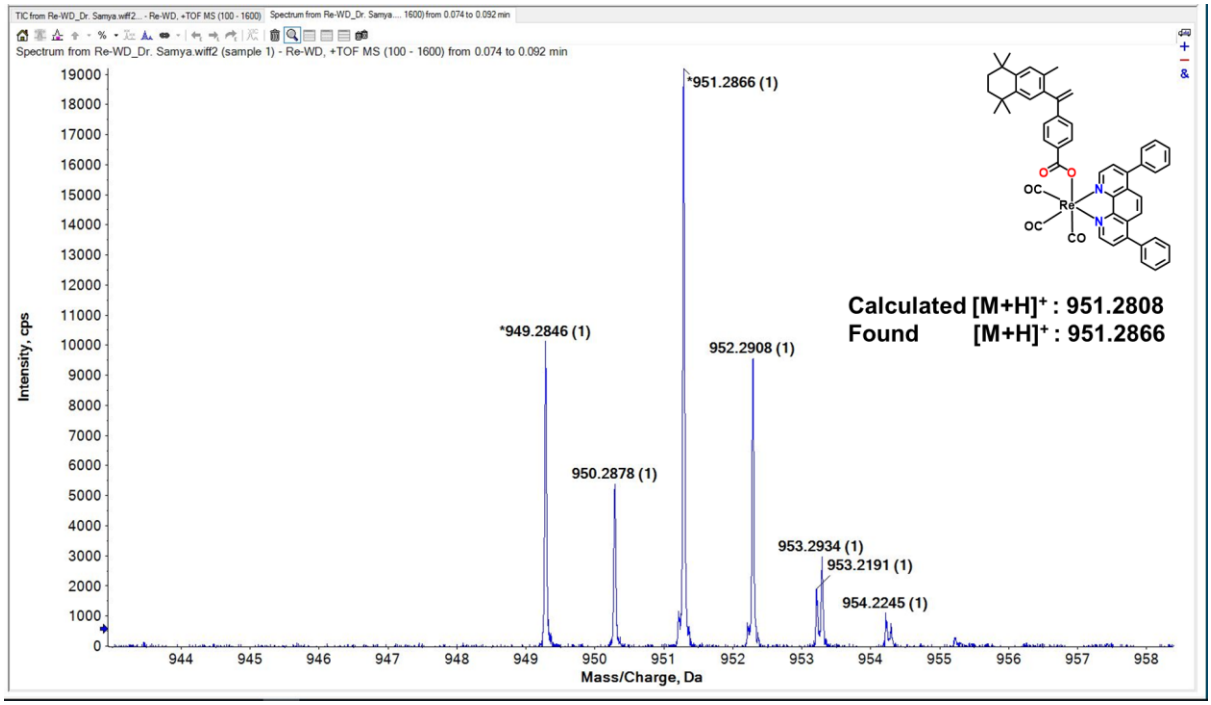

Figure S8: HRMS of **Re2** in CH_3OH.

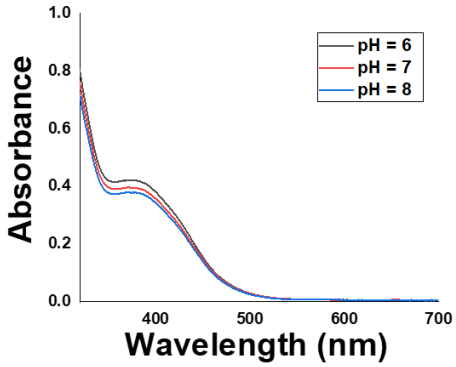

Figure S9: UV-Vis. spectra of **Re2** under different pH conditions.

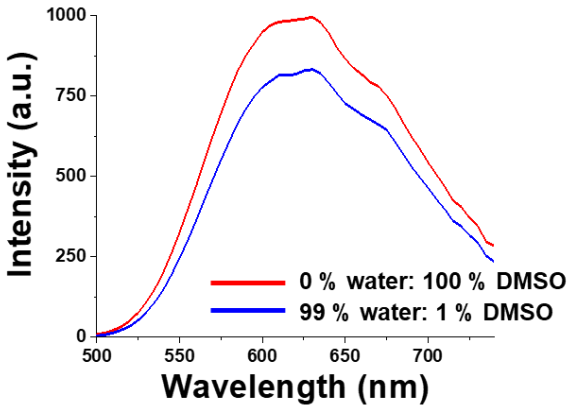

Figure S10: Emission spectra of **Re2** recorded in different DMSO-water (100:0 and 1:99, v/v) solutions, λ_{ex} = 380 nm.

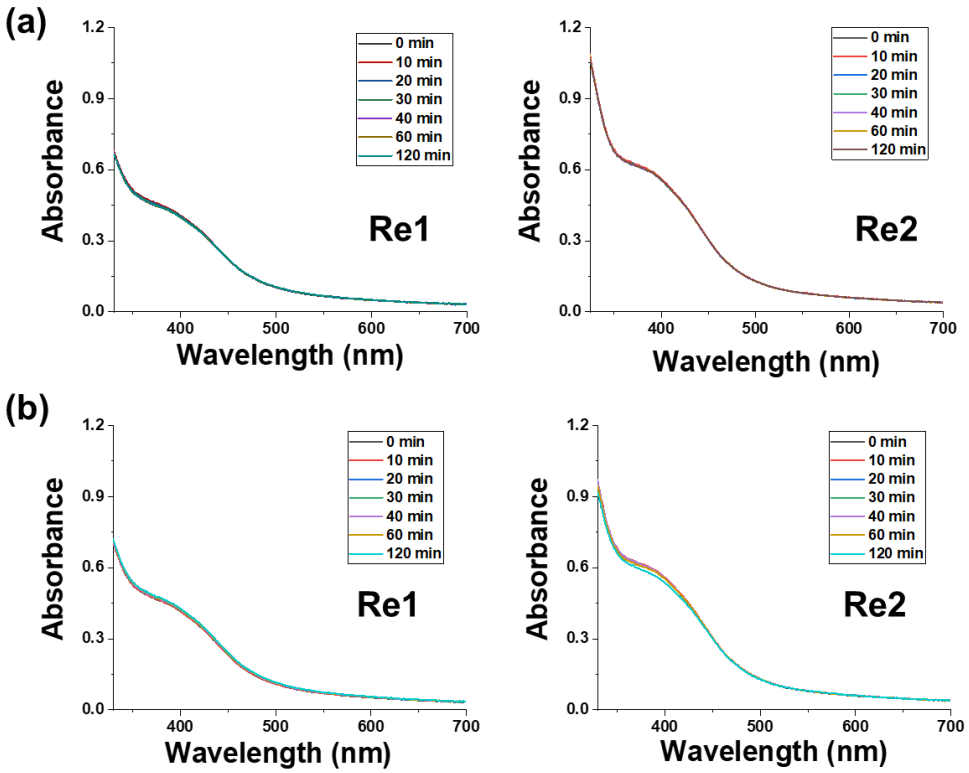

Figure S11. (a) Stability curve for **Re1** and **Re2** in DMSO:DMEM (2:98, v:v) solution under the dark condition. (b) Stability curve for **Re1** and **Re2** in DMSO:DMEM (2:98, v:v) solution under visible light (400-700 nm, 10 J cm^{-2}) exposure.

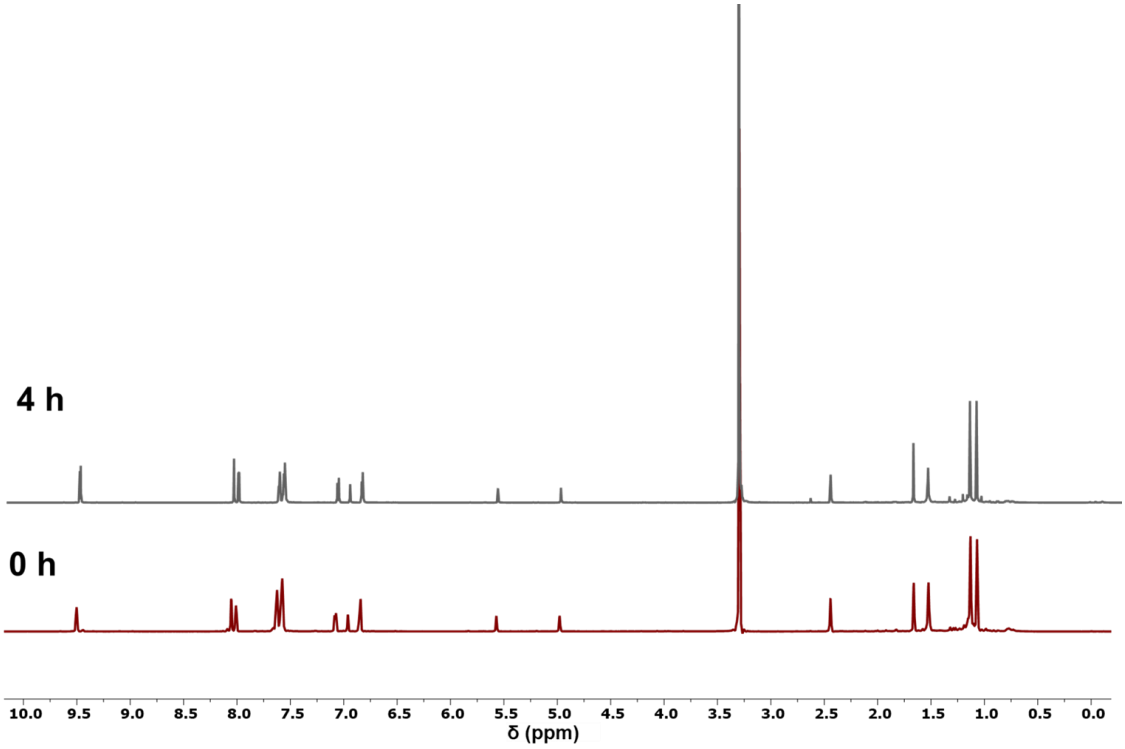

Figure S12. (a) NMR spectra of **Re2** in DMSO-d_6 (500 MHz) solution under visible light (400-700 nm, 10 J cm^{-2}) exposure (4 h) indicating no notable change.

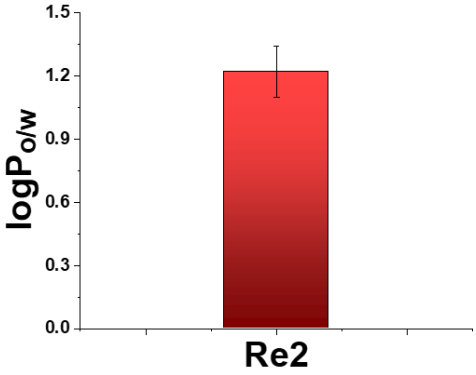

Figure S13. The octanol-water partition coefficient of **Re2.**

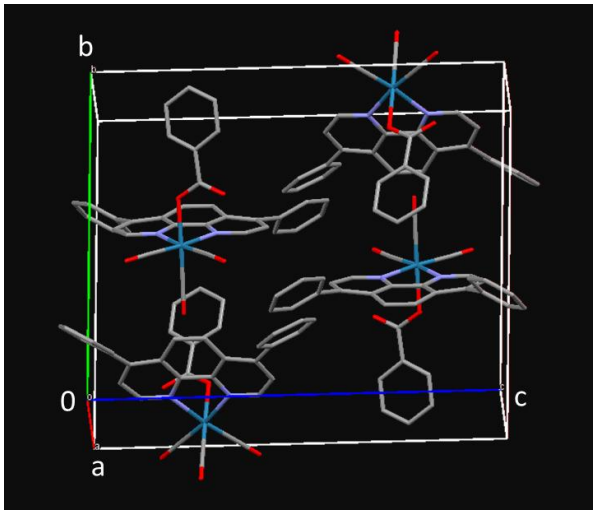

Figure S14. Unit cell packing of **Re1**, drawn by Mercury 3.8**.**

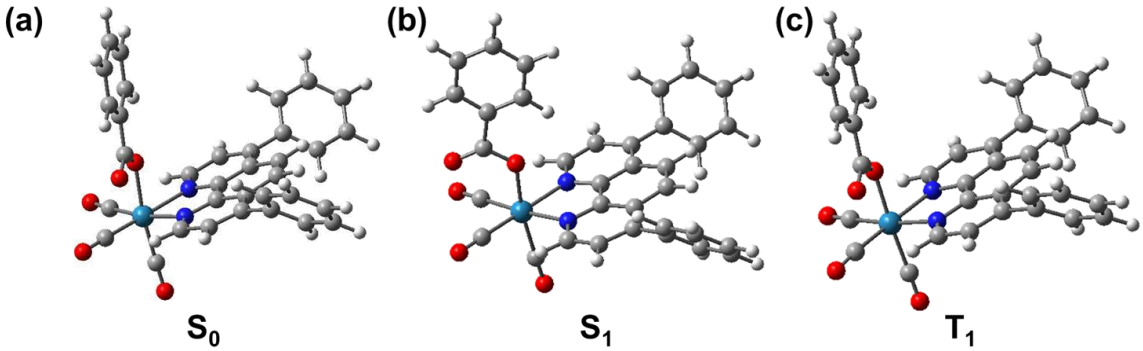

Figure S15: Optimized geometries of **Re1** in water obtained from CAM-B3LYP/LANL2DZ/6-31g* level of theory.

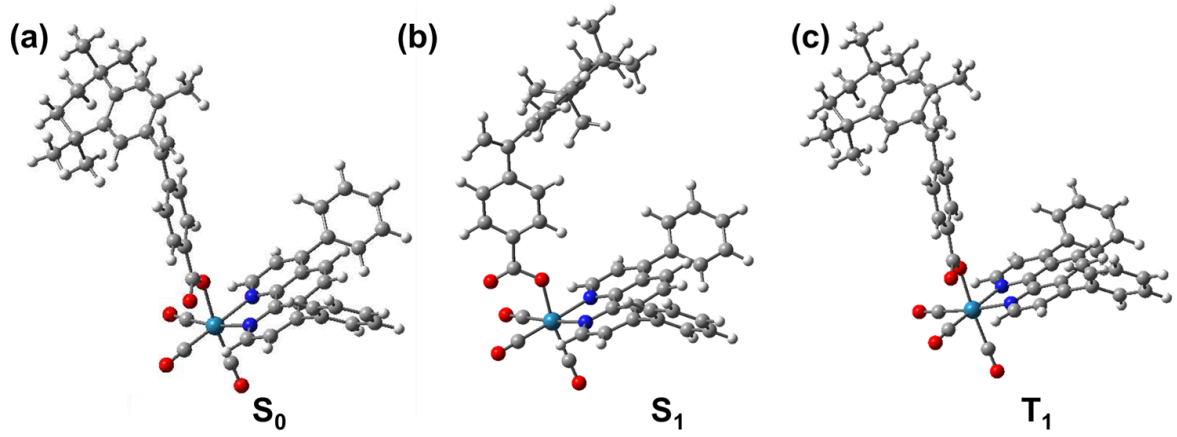

Figure S16: Optimized geometries of **Re2** in water obtained from CAM-B3LYP/LANL2DZ/6-31g* level of theory.

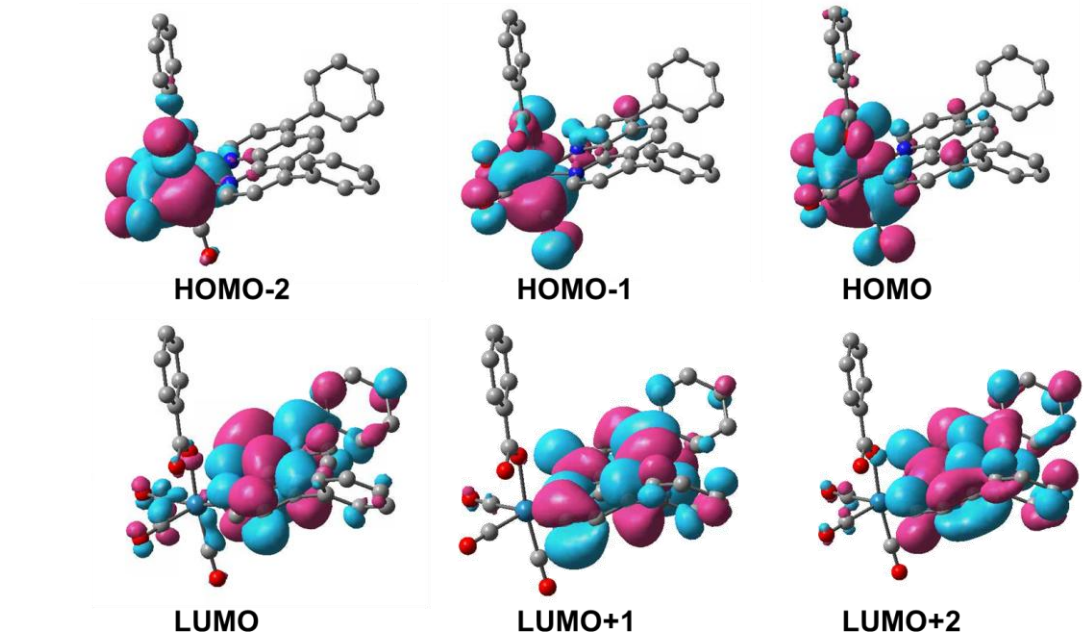

Figure S17: LUMO+1s, LUMOs, HOMOs and HOMO-1s for the **Re1** at S_0 geometry at the CAM-B3LYP/LANL2DZ/6-31g* level of theory. H is omitted for clarity.

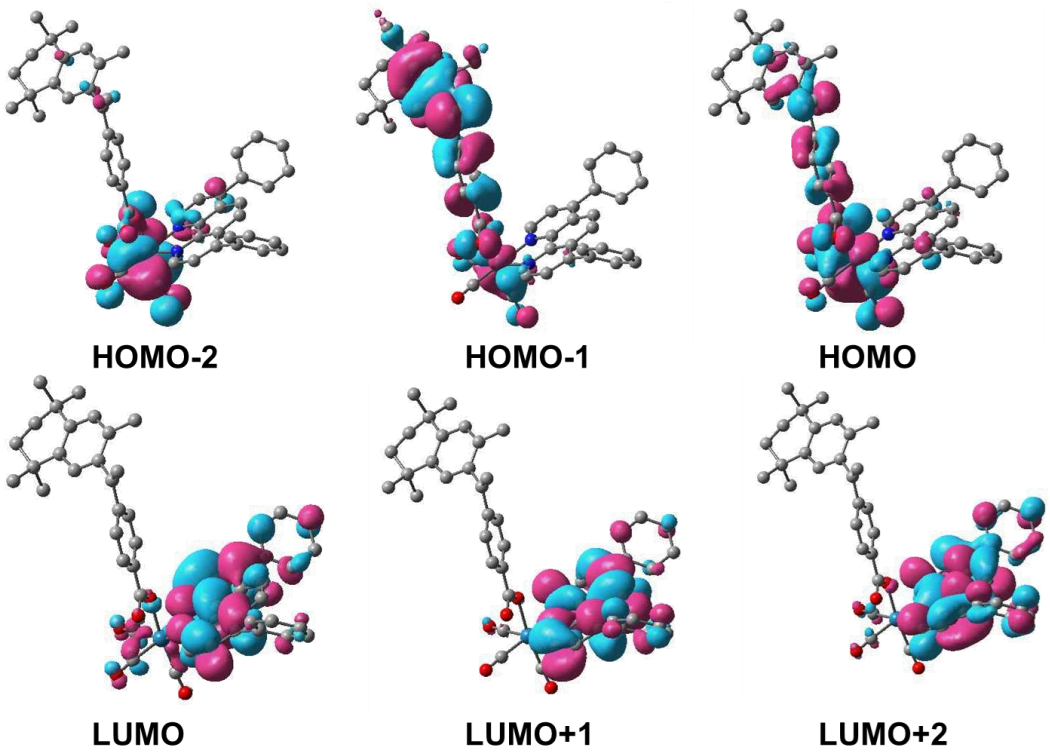

Figure S18: LUMO+1s, LUMOs, HOMOs and HOMO-1s for the **Re2** at S_0 geometry at the CAM-B3LYP/LANL2DZ/6-31g* level of theory. H is omitted for clarity.

Transitions	NTO_o	NTO_v	
$S_0 \rightarrow S_1$	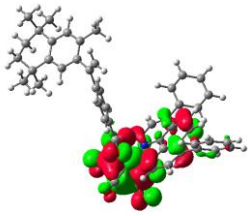	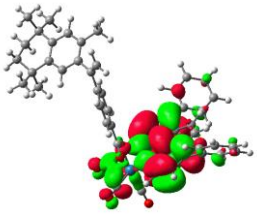	97%
$S_0 \rightarrow S_2$	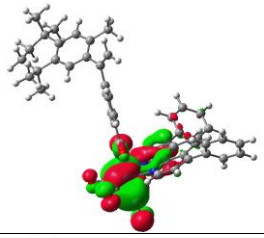	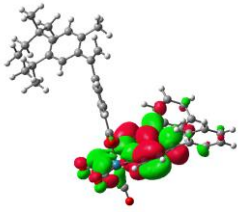	98%
$S_0 \rightarrow S_3$	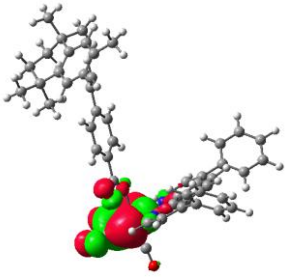	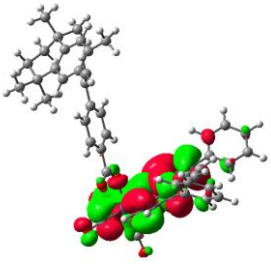	98%

$S_0 \rightarrow S_4$	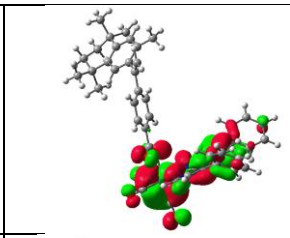	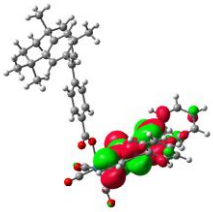	92%
$S_0 \rightarrow S_5$	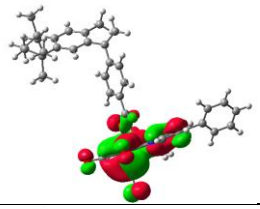	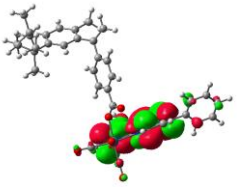	67%
	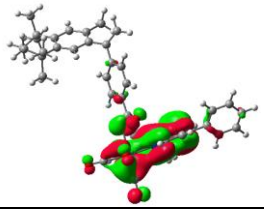	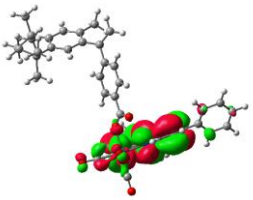	28%

Figure S19: Natural Transition Orbitals (NTOs) for different transitions ($S_0 \rightarrow S_n$; n = 1 to 5) for the **Re2** at CAM-B3LYP/LANL2DZ/6-31g* level of theory in water. The hole (NTO_o) and particle (NTO_v) involved are represented.

Transitions	NTO_o	NTO_v	
$S_0 \rightarrow T_1$	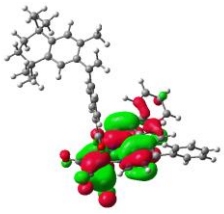	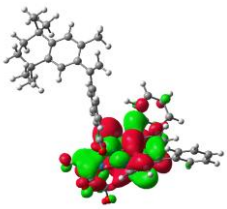	60%
	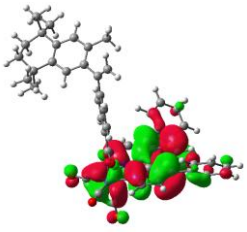	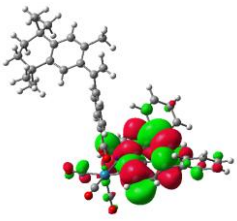	23%
$S_0 \rightarrow T_2$	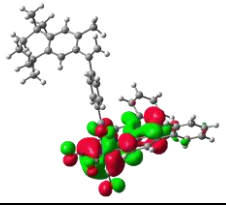	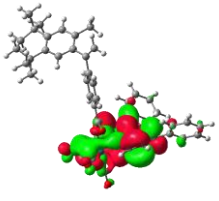	82%

$S_0 \rightarrow T_3$	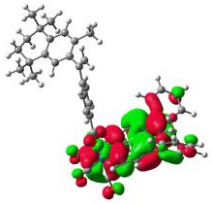	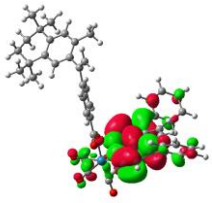	77%
	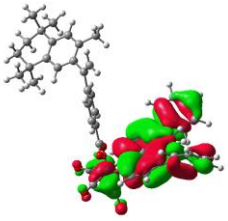	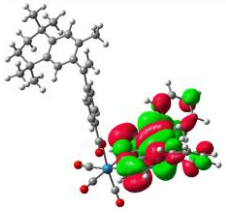	15%
$S_0 \rightarrow T_4$	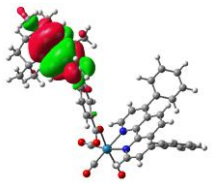	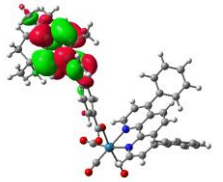	47%
	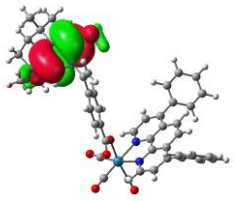	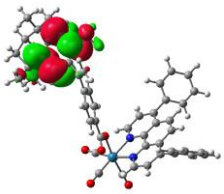	32%
	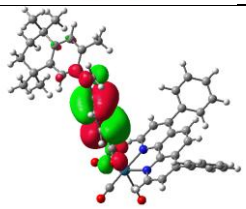	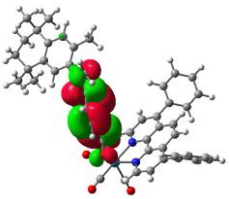	17%
$S_0 \rightarrow T_5$	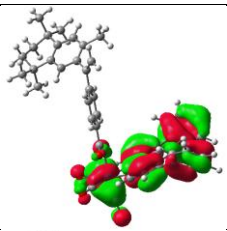	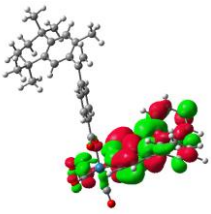	35%
	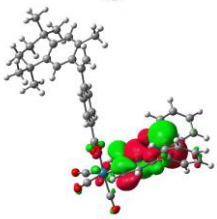	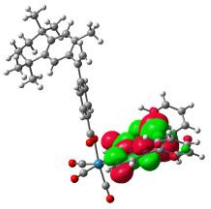	28%
	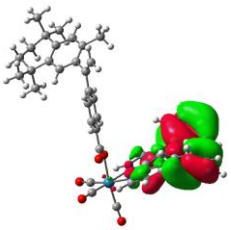	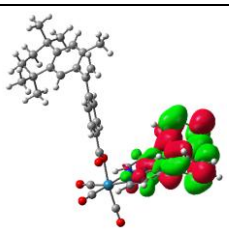	12%

$S_0 \rightarrow T_6$	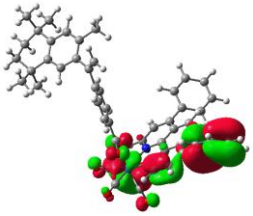	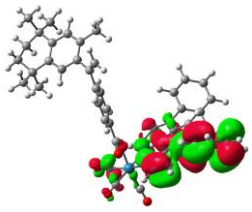	35%
	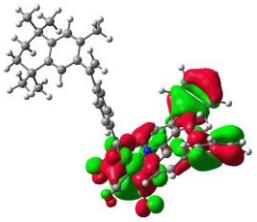	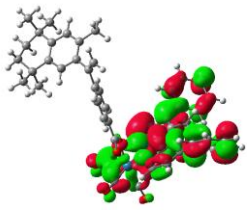	23%
	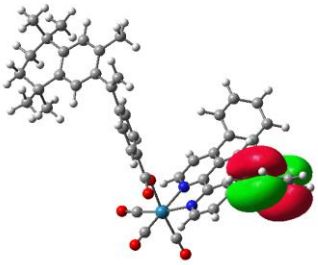	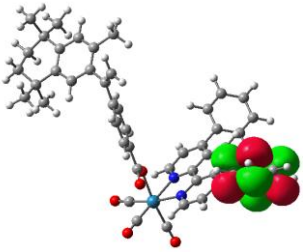	20%
$S_0 \rightarrow T_7$	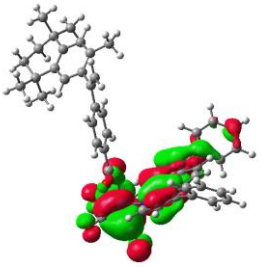	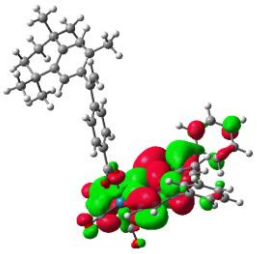	44%
	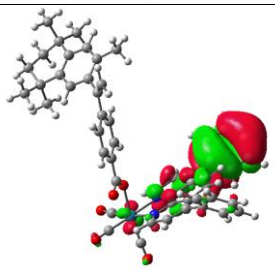	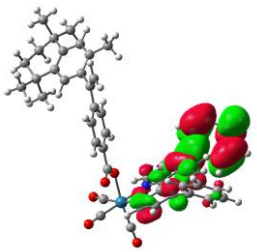	23%
	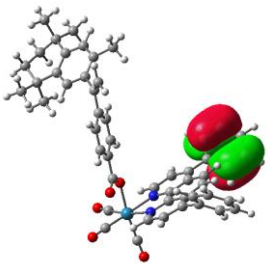	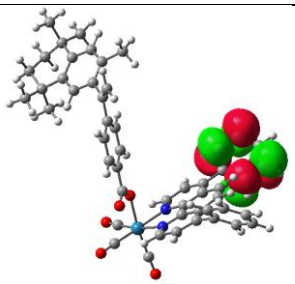	16%
$S_0 \rightarrow T_8$	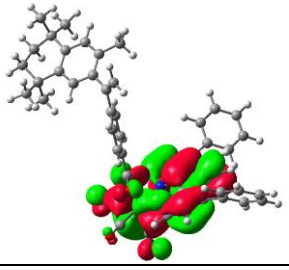	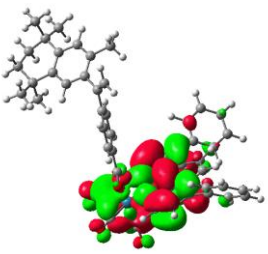	67%

	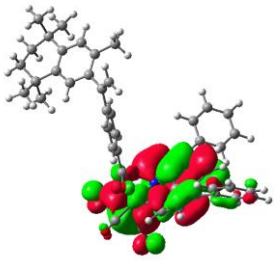	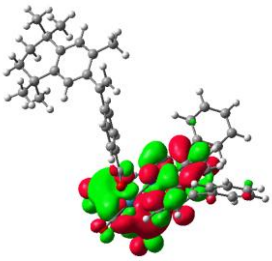	17%
$S_0 \rightarrow T_9$	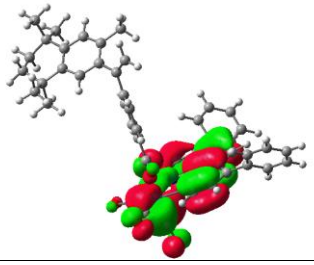	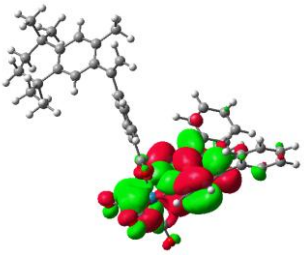	79%
	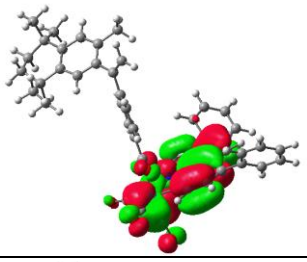	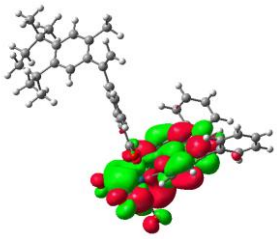	16%
$S_0 \rightarrow T_{10}$	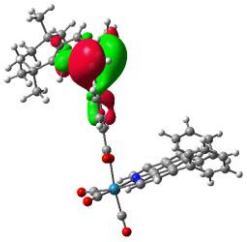	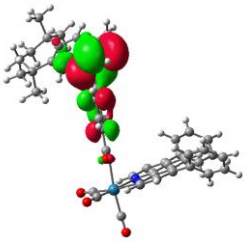	42%
	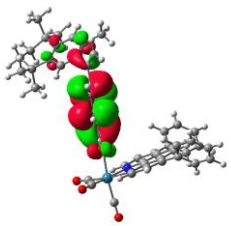	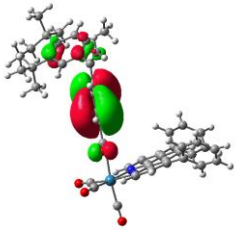	20%
	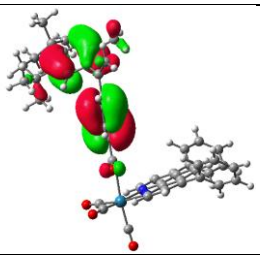	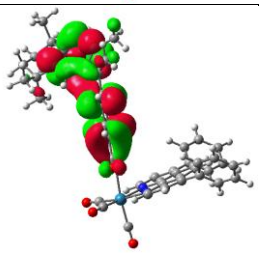	20%

Figure S20: Natural Transition Orbitals (NTOs) for different transitions ($S_0 \rightarrow T_n$, n = 1-10) for the **Re2** at CAM-B3LYP/LANL2DZ/6-31g* level of theory in water. The holes (NTOo) and particles (NTO_v) involved are represented.

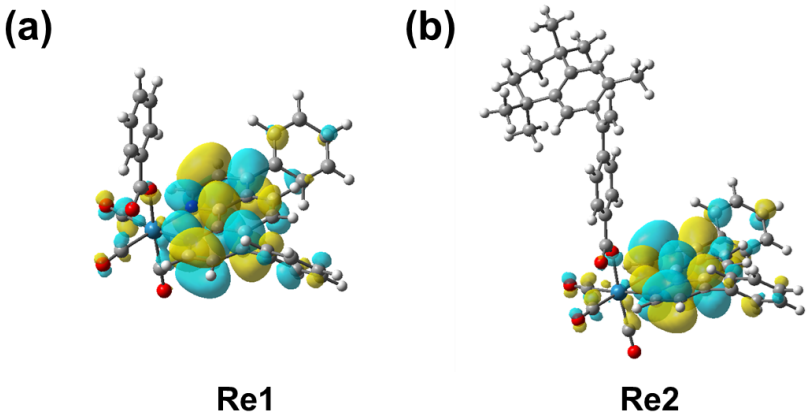

Figure S21: SOMO plots of the triplet excited state of **Re1 (a)** and **Re2 (b)** at CAM-B3LYP/LANL2DZ/6-31g* level of theory in water.

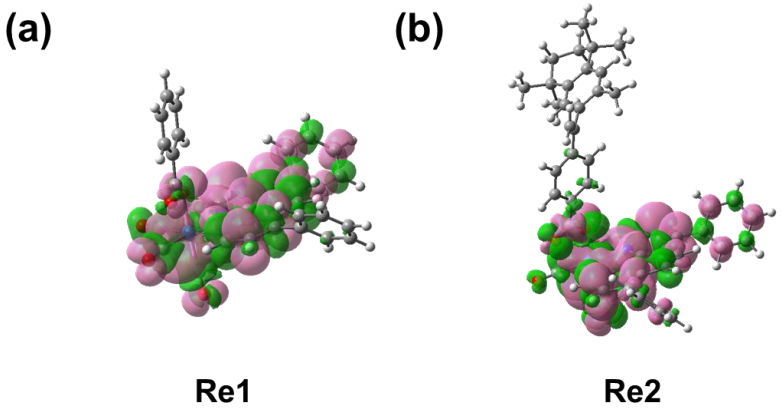

Figure S22: Spin density plots of the triplet excited state of **Re1 (a)** and **Re2 (b)** at CAM-B3LYP/LANL2DZ/6-31g* level of theory in water.

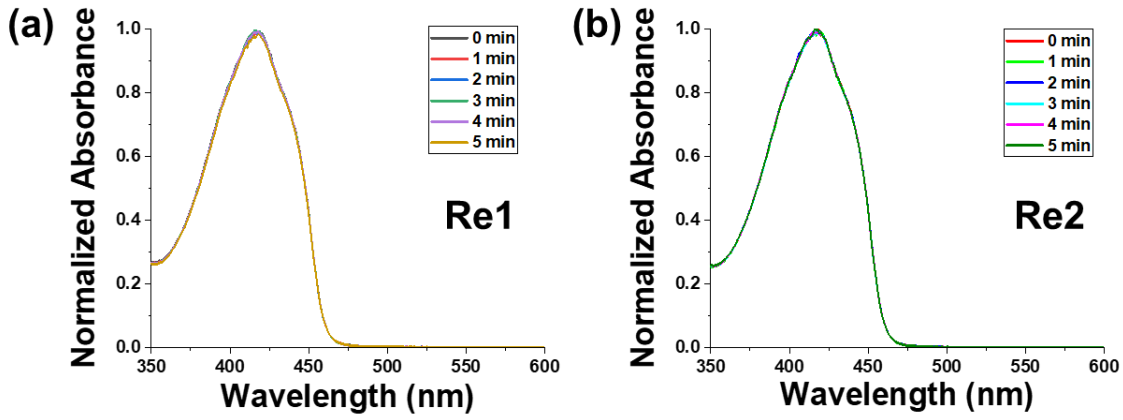

Figure S23: $^1O_2$ generation by (a) **Re1** (2 µM) (b) **Re2** (2 µM) monitored by $^1O_2$ probe, DPBF (50 µM) in DMSO:PBS solution (v/v; 2 : 98) under dark conditions.

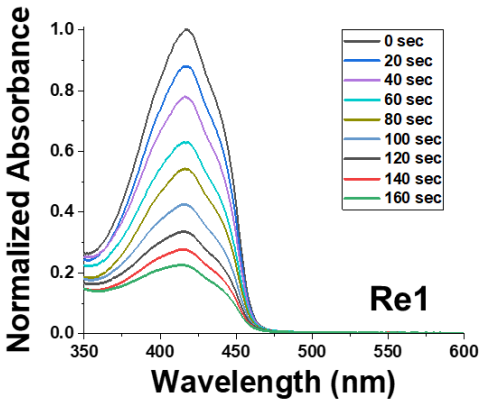

Figure S24: Visible light (400-700 nm) triggered $^1O_2$ generation by **Re1** (2 µM) monitored by using the $^1O_2$ probe, DPBF (50 µM) in DMSO:PBS solution (v/v; 2 : 98).

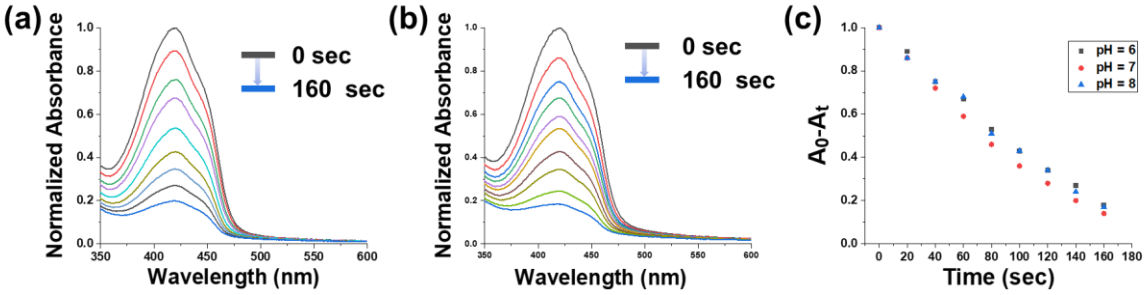

Figure S25: Visible light (400-700 nm) triggered $^1O_2$ generation by **Re2** (2 µM) at different pH conditions; (a) pH = 6, (b) pH = 8 monitored by using the $^1O_2$ probe, DPBF (50 µM).

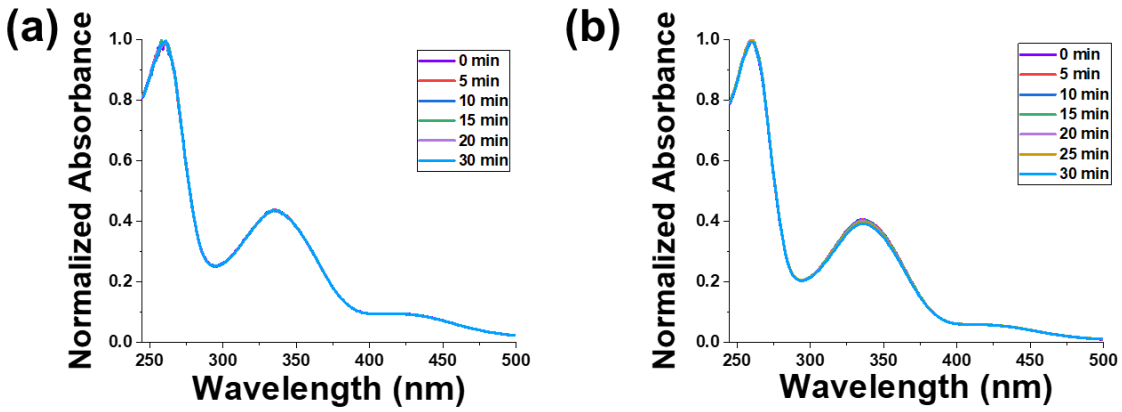

Figure S26: NADH (150 µM) photo-oxidation by (a) **Re1** (5 µM), (b) **Re2** (5 µM) under dark conditions, recorded in DMSO-PBS (2:98 v/v) solution.

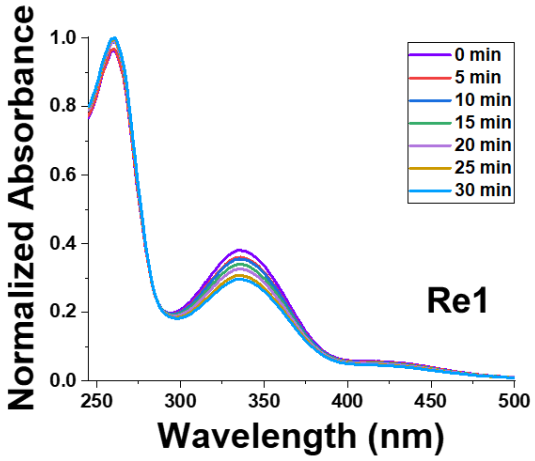

Figure S27: Visible light triggered (400-700 nm) NADH (150 µM) oxidation by **Re1** (5 µM) recorded in DMSO-PBS (2:98 v/v) solution.

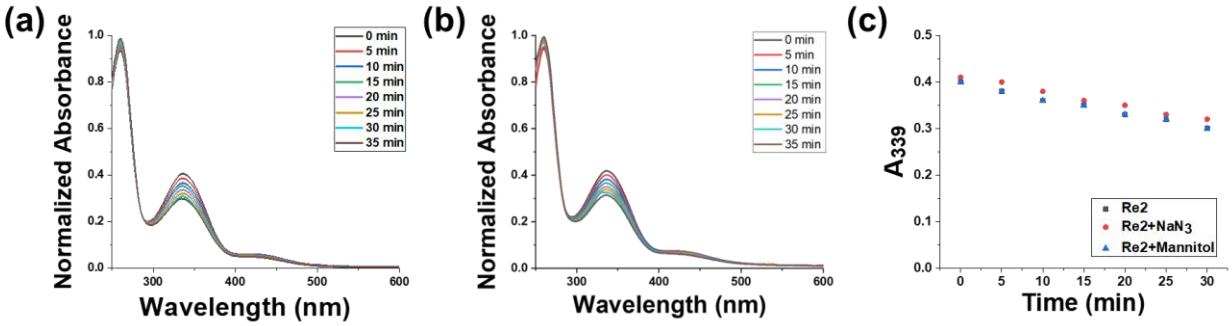

Figure S28: Visible light (400-700 nm) triggered NADH (150 µM) photo-oxidation by **Re2** (5 µM) in the presence of (a) Mannitol (1 mM, ROS scavenger), (b) NaN_3 (1 mM, $^1O_2$ scavenger), recorded in DMSO-PBS (2:98 v/v) solution. (c) A decrease in NADH-based peak (339 nm) over time, indicating similar NADH photo-oxidation in the presence of different ROS scavengers.

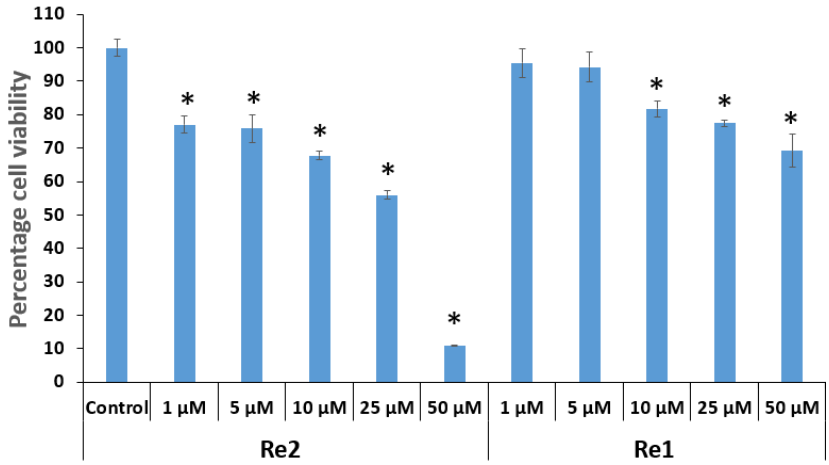

Figure S29: Cell viability plots for **Re1** and **Re2** in A549 cells under dark conditions. Where * denotes statistically significant ($p<0.05$).

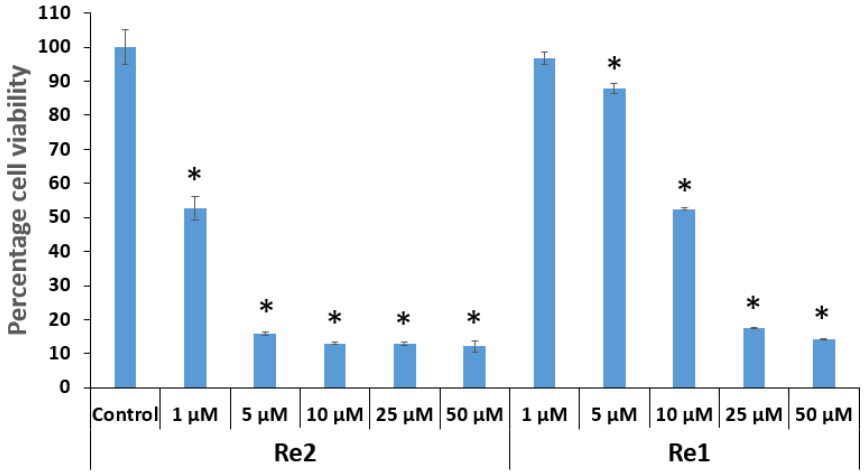

Figure S30: Cell viability plots for **Re1** and **Re2** in A549 cells under light irradiation (λ= 400-700 nm, 10 J cm^{-2}). Where * denotes statistically significant ($p<0.05$).

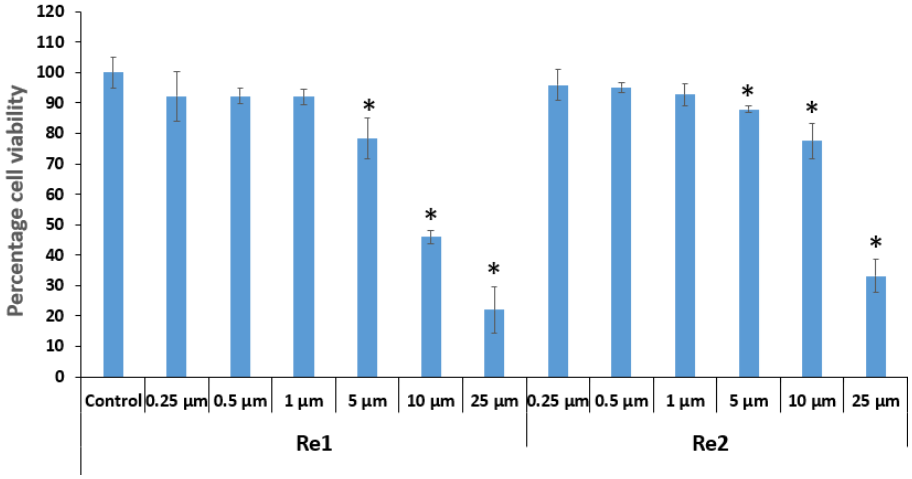

Figure S31: Cell viability plots for **Re1** and **Re2** in MCF-7 cells under dark conditions. Where * denotes statistically significant ($p<0.05$).

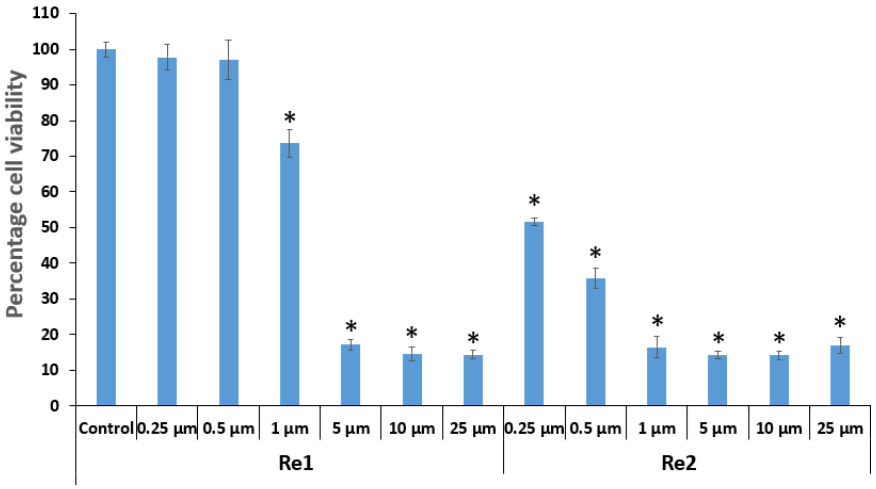

Figure S32: Cell viability plots for **Re1** and **Re2** in MCF-7 cells under light irradiation (λ= 400-700 nm, 10 J cm^{-2}). Where * denotes statistically significant ($p<0.05$).

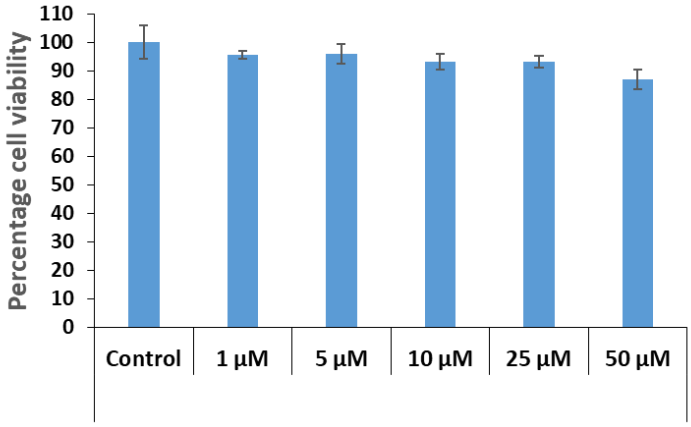

Figure S33: Cell viability plot using MTT assay for complex **Re2** in HEK-293 cells under dark conditions.

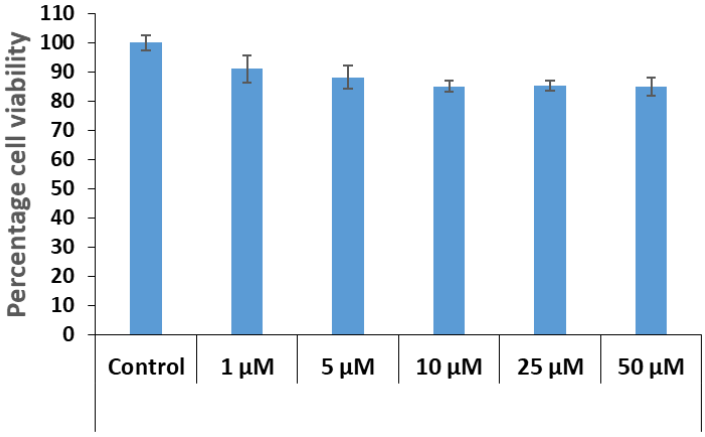

Figure S34: Cell viability plot using MTT assay for complex **Re2** in HEK-293 cells under light (λ= 400-700 nm, 10 J cm^{-2}) conditions.

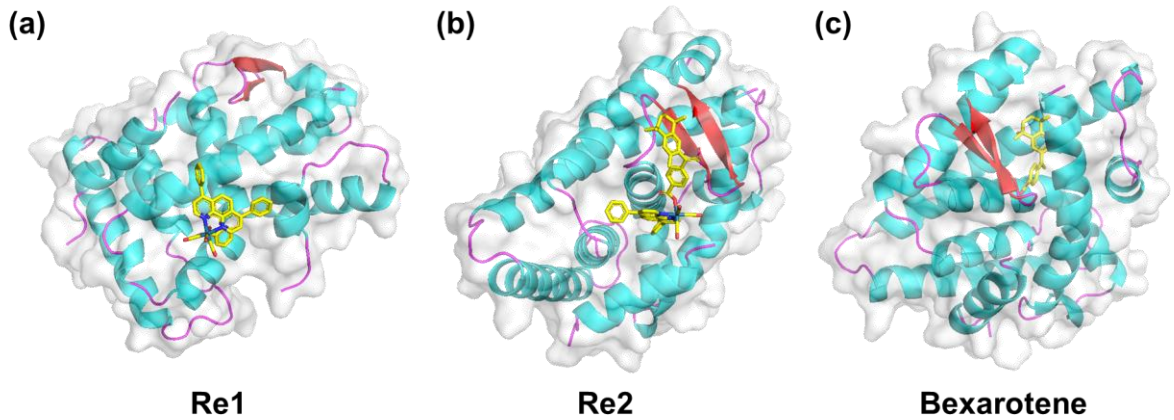

Figure S35: Domain architecture of the (a) Re1, (b) **Re2**, (c) bexarotene-docked structure with RXRα receptor (PDB ID: 1MVC) obtained by molecular docking.

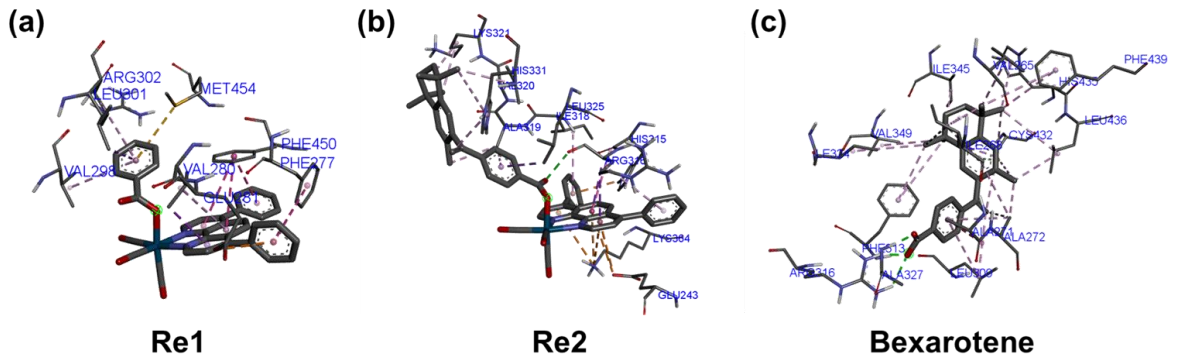

Figure S36: Interaction of (a) **Re1**, (b) **Re2**, (c) bexarotene with RXRα receptor (PDB ID: 1MVC).

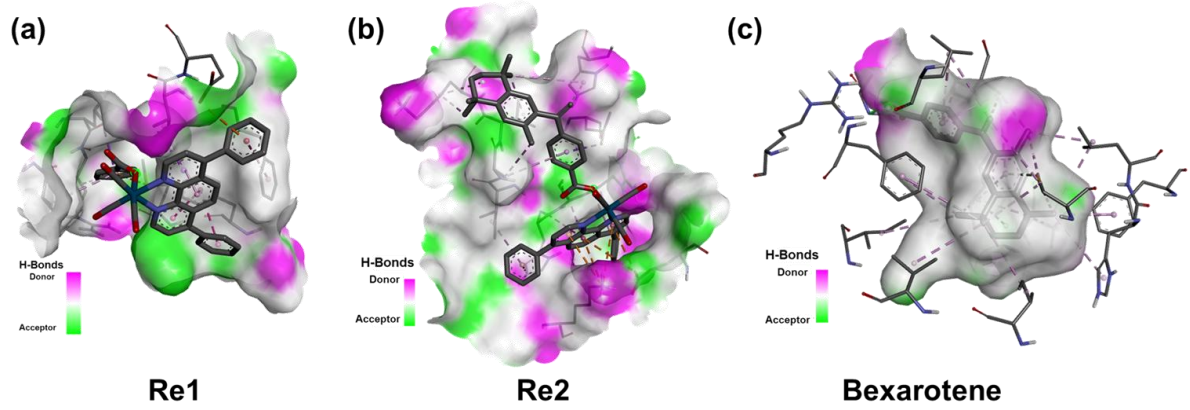

Fig. S37: Interaction of (a) **Re1**, (b) **Re2**, (c) bexarotene with the H-bond receptor surface of RXRα receptor (PDB ID: 1MVC).

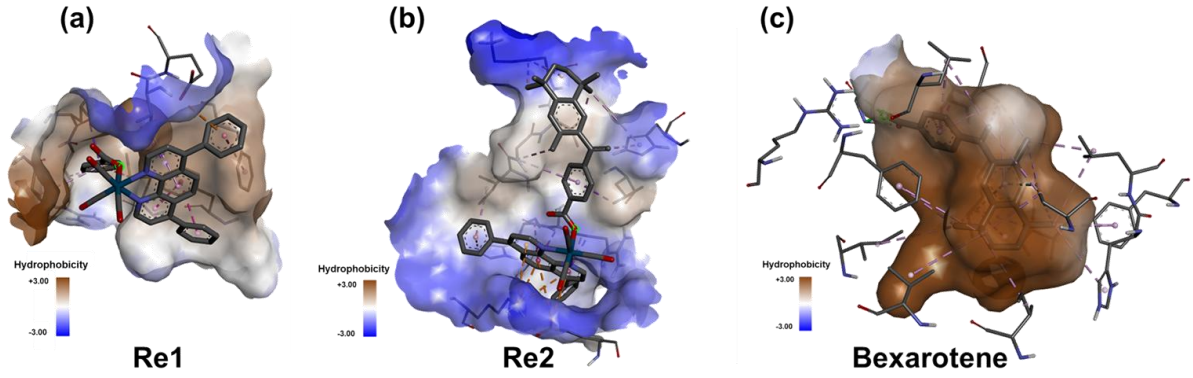

Figure S38: Interaction of (a) **Re1**, (b) **Re2**, (c) bexarotene with the H-bond receptor surface of RXRα receptor (PDB ID: 1MVC).

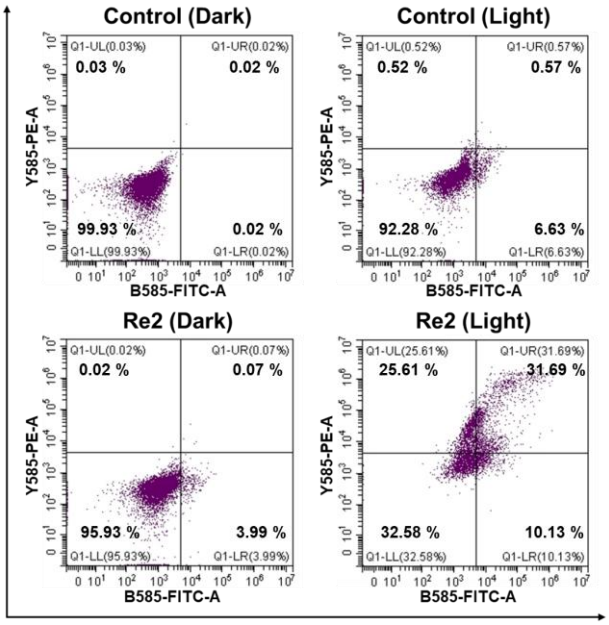

Figure S39. Quantitative determination of apoptosis induced by **Re2** in MCF-7 cells using Annexin V/FITC and PI assay

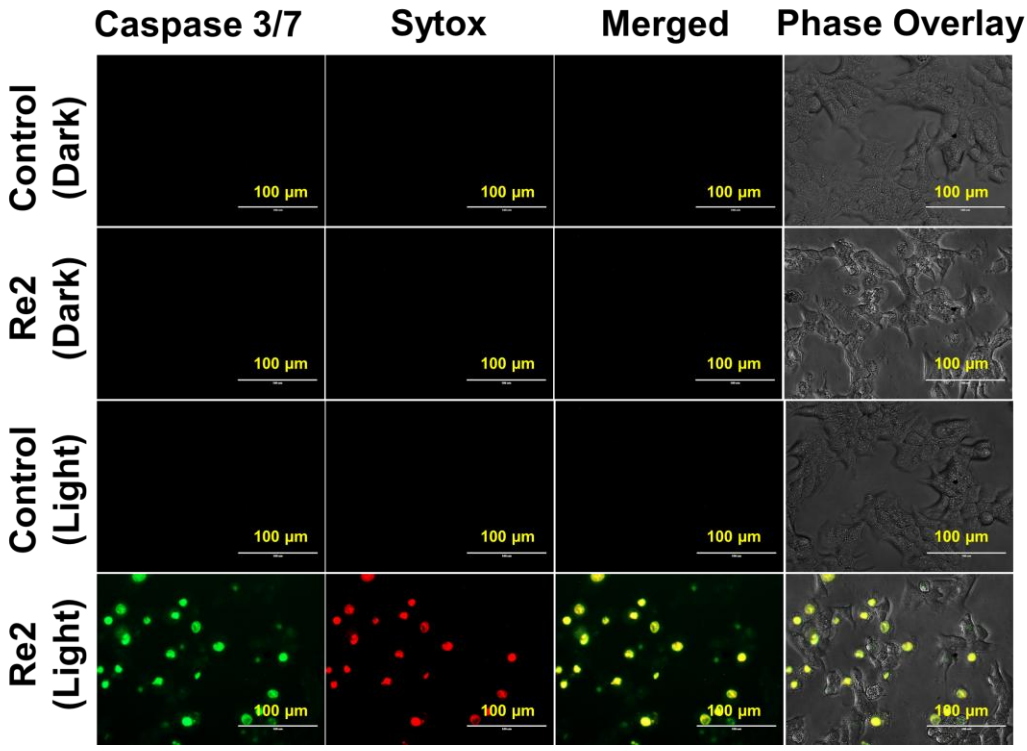

Figure S40: Caspase 3/7 and SYTOX red assay. The merged panel indicates the caspase activation induced in MCF-7 cells by **Re2** in the presence of light exposure. scale bar: 100 µm. Incubation time: 12 h.

.

Optimized ground state Coordinates

Re1

C	-1.21961	-2.53	-3.03087
N	-1.14638	-3.40554	-1.98605
C	-0.0046	-3.48161	-1.28235
C	1.13901	-2.69856	-1.55351
C	1.11922	-1.7448	-2.61196
C	-0.10718	-1.65768	-3.34082
C	-0.0304	-4.36812	-0.20007
C	1.08505	-4.55563	0.6099
C	2.24805	-3.80343	0.34029
C	2.27638	-2.88161	-0.74271
N	-1.175	-5.03621	0.01078
C	-1.30308	-5.91919	1.00618
C	-0.23036	-6.13662	1.89251
C	0.98906	-5.46103	1.69258
C	2.40187	-0.82095	-2.92205
C	2.18063	-5.71309	2.65612
C	1.9608	-5.97293	3.97654
C	3.15546	-6.14009	4.94332
C	4.42317	-6.10291	4.46754
C	4.67108	-5.8859	2.96465
C	3.62631	-5.67514	2.1236
C	3.71078	-1.35768	-2.7971
C	4.86161	-0.56998	-3.0545
C	4.74092	0.7807	-3.3872
C	3.46733	1.34495	-3.51486
C	2.29876	0.5485	-3.32795
Re	-2.57911	-4.69377	-1.33123

O	-3.427	-3.14309	-0.37635
C	-3.96523	-3.33354	0.98757
O	-3.92578	-4.46794	1.53105
C	-4.60221	-2.1017	1.77627
C	-3.82248	-1.39693	2.71432
C	-4.34857	-0.27902	3.42047
C	-5.68065	0.15944	3.21558
C	-6.46718	-0.5335	2.28053
C	-5.93807	-1.64977	1.56034
C	-4.1495	-4.55309	-2.6524
O	-5.02288	-4.49594	-3.3472
C	-3.90313	-5.99548	-0.44196
O	-4.63238	-6.70322	0.02808
C	-1.66628	-6.22958	-2.32451
O	-1.16592	-7.0714	-2.86898
H	-2.11752	-2.4775	-3.61635
H	-0.19553	-0.95392	-4.14475
H	3.11504	-3.92907	0.95167
H	3.15801	-2.30484	-0.92812
H	-2.22104	-6.46419	1.12786
H	-0.3362	-6.82594	2.70321
H	0.96122	-6.04596	4.35095
H	2.98416	-6.28071	5.99169
H	5.2514	-6.23013	5.1353
H	5.67048	-5.899	2.58254
H	3.80696	-5.49666	1.08516
H	3.83647	-2.37748	-2.51379
H	5.83825	-1.01001	-2.9974
H	5.6218	1.38063	-3.54317

H	3.38195	2.38886	-3.75504
H	1.34081	0.99904	-3.47495
H	-2.81574	-1.70874	2.89279
H	-3.72352	0.23703	4.12127
H	-7.47616	-0.21654	2.11303
H	-6.56318	-2.15064	0.8508
H	-6.07548	0.99356	3.7571

Re2

C	-1.21961	-2.53	-3.03087
N	-1.14638	-3.40554	-1.98605
C	-0.0046	-3.48161	-1.28235
C	1.13901	-2.69856	-1.55351
C	1.11922	-1.7448	-2.61196
C	-0.10718	-1.65768	-3.34082
C	-0.0304	-4.36812	-0.20007
C	1.08505	-4.55563	0.6099
C	2.24805	-3.80343	0.34029
C	2.27638	-2.88161	-0.74271
N	-1.175	-5.03621	0.01078
C	-1.30308	-5.91919	1.00618
C	-0.23036	-6.13662	1.89251
C	0.98906	-5.46103	1.69258
C	2.40187	-0.82095	-2.92205
C	2.18063	-5.71309	2.65612
C	1.9608	-5.97293	3.97654
C	3.15546	-6.14009	4.94332
C	4.42317	-6.10291	4.46754
C	4.67108	-5.8859	2.96465

C	3.62631	-5.67514	2.1236
C	3.71078	-1.35768	-2.7971
C	4.86161	-0.56998	-3.0545
C	4.74092	0.7807	-3.3872
C	3.46733	1.34495	-3.51486
C	2.29876	0.5485	-3.32795
Re	-2.57911	-4.69377	-1.33123
O	-3.427	-3.14309	-0.37635
C	-3.96523	-3.33354	0.98757
O	-3.92578	-4.46794	1.53105
C	-4.60221	-2.1017	1.77627
C	-3.82248	-1.39693	2.71432
C	-4.34857	-0.27902	3.42047
C	-5.68065	0.15944	3.21558
C	-6.46718	-0.5335	2.28053
C	-5.93807	-1.64977	1.56034
C	-6.25443	1.38857	4.02719
C	-7.74244	1.90227	3.872
C	-5.42659	2.01821	4.91419
C	-8.21574	2.97857	4.65653
C	-9.56921	3.3813	4.56839
C	-10.51937	2.63617	3.8261
C	-10.05308	1.52586	3.0273
C	-8.64141	1.27325	2.97362
C	-12.00877	3.03962	4.02756
C	-12.2186	2.82421	2.54054
C	-12.12027	1.40433	1.97331
C	-10.93612	0.42284	2.30852
C	-7.26867	3.71515	5.64154

C	-13.16373	4.04154	3.79434
C	-11.53728	4.19986	4.92623
C	-9.53628	0.0397	1.77011
C	-11.44963	-0.03804	0.92817
C	-4.1495	-4.55309	-2.6524
O	-5.02288	-4.49594	-3.3472
C	-3.90313	-5.99548	-0.44196
O	-4.63238	-6.70322	0.02808
C	-1.66628	-6.22958	-2.32451
O	-1.16592	-7.0714	-2.86898
H	-2.11752	-2.4775	-3.61635
H	-0.19553	-0.95392	-4.14475
H	3.11504	-3.92907	0.95167
H	3.15801	-2.30484	-0.92812
H	-2.22104	-6.46419	1.12786
H	-0.3362	-6.82594	2.70321
H	0.96122	-6.04596	4.35095
H	2.98416	-6.28071	5.99169
H	5.2514	-6.23013	5.1353
H	5.67048	-5.899	2.58254
H	3.80696	-5.49666	1.08516
H	3.83647	-2.37748	-2.51379
H	5.83825	-1.01001	-2.9974
H	5.6218	1.38063	-3.54317
H	3.38195	2.38886	-3.75504
H	1.34081	0.99904	-3.47495
H	-2.81574	-1.70874	2.89279
H	-3.72352	0.23703	4.12127
H	-7.47616	-0.21654	2.11303

H	-6.56318	-2.15064	0.8508
H	-4.42052	1.67227	5.04506
H	-5.77879	2.85034	5.49175
H	-9.8896	4.25896	5.08782
H	-8.25608	0.57193	2.26563
H	-11.47266	3.4301	2.06208
H	-13.20141	3.17081	2.28641
H	-12.10887	1.54626	0.90728
H	-13.00492	0.88268	2.27533
H	-7.58623	4.73215	5.75724
H	-7.29777	3.22484	6.59538
H	-6.26919	3.6961	5.2625
H	-13.37529	4.118	2.75089
H	-14.03996	3.68978	4.31062
H	-12.89049	5.0015	4.17495
H	-12.15097	5.06168	4.73396
H	-11.61092	3.93299	5.953
H	-10.5176	4.43451	4.68779
H	-8.89485	-0.2154	2.58427
H	-9.12105	0.85651	1.22424
H	-9.63275	-0.81171	1.11599
H	-11.20069	-0.74733	0.16061
H	-10.57245	0.46503	0.5784
H	-11.74972	-0.91406	1.46658

References:

1. N. Montesdeoca, L. Johannknecht, E. Efanova, J. Heinen-Weiler and J. Karges, *Angew. Chem. Int. Ed.*, 2024, **63**, e202412585.
2. M. J. Frisch, G. W. Trucks, H. B. Schlegel, G. E. Scuseria, J. R. Cheeseman, G. Scalmani, S. V. Barone, G. A. Petersson, H. Nakatsuji, X. Li, M. Caricato, A. V. Marenich, J. Bloino, B. G. Janesko, R. Gomperts, B. Mennucci, H. P. Hratchian, J. V. Ortiz, A. F. Izmaylov, J. L. Sonnenberg, D. Williams-Young, F. Ding, F. Lipparini, F. Egidi, J. Goings, B. Peng, A.

Petrone, T. Henderson, D. Ranasinghe, V. G. Zakrzewski, J. Gao, N. Rega, G. Zheng, W. Liang, M. Hada, M. Ehara, K. Toyota, R. Fukuda, J. -4 -2 0 2 0 50 100 Dark Light S26 Hasegawa, M. Ishida, T. Nakajima, Y. Honda, O. Kitao, H. Nakai, T. Vreven, K. Throssell, J. A. Montgomery Jr., J. E. Peralta, F. Ogliaro, M. J. Bearpark, J. J. Heyd, E. N. Brothers, K. N. Kudin, V. N. Staroverov, T. A. Keith, R. Kobayashi, J. Normand, K. Raghavachari, A. P. Rendell, J. C. Burant, S. S. Iyengar, J. Tomasi, M. Cossi, J. M. Millam, M. Klene, C. Adamo, R. Cammi, J. W. Ochterski, R. L. Martin, K. Morokuma, O. Farkas, J. B. Foresman, and D. J. Fox, Gaussian 16 Rev. A.03, Wallingford, CT, 2016.

3. S. G. Chiodo, N. Russo and E. Sicilia, *J. Chem. Phys.* 2006, **125**, 104107-104115.
4. L. V. Lutkus, S. S. Rickenbach and T. M. McCormick, *J. Photochem. Photobiol. A*, 2013, **378**, 131-135.
5. T. Entradasa, S. Waldrona and M. Volk, *J. Photochem. Photobiol. B.*, 2020, **204**, 111787.
6. H. Huang, S. Banerjee, K. Qiu, P. Zhang, O. Blacque, T. Malcomson, M. J. Paterson, G. J. Clarkson, M. Staniforth, V. G. Stavros, G. Gasser, H. Chao and P. J. Sadler, *Nat. Chem.*, 2019, **11**, 1041-1048.
7. G. M. Morris, R. Huey, W. Lindstrom, M. F. Sanner, R. K. Belew, D. S. Goodsell, A. J. Olson, *J. Comput. Chem.,* 2009, **16**, 2785-91.
8. M. K. Bitew, T. Desalegn, T. B. Demissie, A. Belayneh, M. Endale and R. Eswaramoorthy, *PLoS One*, 2021, **16**, e0260853.
9. Dassault Systèmes BIOVIA. Discovery Studio Modeling Environment, Release 2017.
10. Dassault Systèmes; San Diego, CA, USA: 2017. 10. R. E. Rigsby and A. B. Parker, Biochem. *Mol. Biol. Educ.,* 2016, **44**, 433−437.
11. J. van Meerloo , G. J. Kaspers and J. Cloos , *Methods Mol. Biol.*, 2011, **731**, 237-245.
12. A. K. Mehata, V. Singh, Vikas, N. Singh, A. Mandal, D. Dash, B. Koch and M. S. Muthu, *ACS Appl. Mater. Interfaces,* 2023, **15**, 34343-34359.
13. R. Kushwaha, A. Upadhyay, S. Peters, A. K. Yadav, A. Mishra, A. Bera, T. Sadhukhan and S. Banerjee, *Langmuir*, 2024, **40**, 12226-12238
14. A. Paul, P. Singh, M. L. Kuznetsov, A. Karmakar, M. F. C. G. D. Silva, B. Koch and A. J. L. Pombeiro, *Dalton Trans.*, 2021, **50**, 3701-3716.
15. A. K. Yadav, V. Singh, S. Acharjee, S. Saha, R. Kushwaha, A. Dutta, B. Koch and S. Banerjee, *Chem. Eur. J.,* 2025, **31**, e202403454.